# Coupled-mode theory for optical waveguides: an overview

**Wei-Ping Huang**

*Department of Electrical and Computer Engineering, University of Waterloo, Waterloo, Ontario N2L 3G1, Canada*

Received October 23, 1992; revised manuscript received August 10, 1993; accepted August 10, 1993

The coupled-mode theory (CMT) for optical waveguides is reviewed, with emphasis on the analysis of coupled optical waveguides. A brief account of the recent development of the CMT for coupled optical waveguides is given. Issues raised in the debates of the 1980's on the merits and shortcomings of the conventional as well as the improved coupled-mode formulations are discussed. The conventional coupled-mode formulations are set up in a simple, intuitive way. The rigorous CMT is established on the basis of a linear superposition of the modes for individual waveguides. The cross-power terms appear logically as a result of modal nonorthogonality. The cross power is necessary for the self-consistency of the CMT for dissimilar waveguides. The nonorthogonal CMT, though more complicated, yields more-accurate results than the conventional orthogonal CMT for most practical applications. It also leads to the prediction of cross talk in directional couplers. The conventional orthogonal CMT is, however, reliably accurate for describing the power coupling between two weakly coupled, nearly identical waveguides. For dissimilar waveguides, a self-consistent orthogonal CMT can be derived by a redefinition of the coupling coefficients, and it predicts the coupling length and therefore the power exchange between the waveguides accurately if the two waveguides are far apart. Three typical coupler configurations—the uniform, the grating-assisted, and the tapered—are examined in detail. The accuracy, scope of validity, limitations, and extensions of the coupled-mode formulations are discussed in conjunction with each configuration. To verify the arguments in the discussions, comparisons with the exact analytical solutions and the rigorous numerical simulations are made.

## 1. INTRODUCTION

Coupled-mode theory (CMT) has been applied extensively in guided-wave optics as a mathematical tool for the analysis of electromagnetic wave propagation and interaction with media. Because of its mathematical simplicity and physical intuitiveness, the CMT is a fruitful approach to an understanding of the operation of existing devices and systems as well as in the suggestion of new concepts and designs. The literature on the theoretical and practical aspects of the CMT is vast; for a general review of the principal features of the theory, one may refer to the recent review paper by Haus and Huang[1] and the references therein. There are also several excellent reference books available on the subject.[2–8] The focus of this paper is primarily on the coupled-mode theory for guided-wave optics, with emphasis on optical guided-wave devices that are based on coupled waveguides. In particular, I concentrate on the development of the theory in the past seven years. There have been substantial interest and research activities related to the CMT in this period, as reflected by the large number of publications on the subject.

There are a number of different coupled-mode formulations in the literature. The choice of a particular formulation depends on the problems examined, on the accuracy desired, and sometimes on the preference of the user. It is beyond the scope of this paper to discuss all the formulations. Instead, I deal with the coupled-mode formulations that are based on ideal or local modes of the individual waveguides for three typical coupler structures. The waveguiding media are assumed to be isotropic, linear, and lossless. The above choices of the modes and the media may not be appropriate for some practical situations. However, the principal features of the CMT are similar for the other formulations, as well. One of the major topics to be discussed is the distinction and the relation between the conventional orthogonal and the improved nonorthogonal CMT's. Issues related to the advantages and the disadvantages of the two theories have been debated and are yet to be completely settled. In the broader view, questions still remain about the accuracy and the scope of validity of the coupled-mode theory for the analysis of coupled optical waveguides. It is the hope of the author that the passage of time would permit the production of a paper that could put the topic of the coupled-mode theory for coupled optical waveguides into perspective. To achieve this objective, effort has been made to give a brief and objective account of the debates that occurred in the late 1980's and to summarize the conclusions that have been drawn and whatever controversial issues remain, at least from the author's point of view. The paper follows a systematic derivation of the coupled-mode theory based on the modes of individual waveguides, so that one is able to judge and appreciate the assumptions, the approximations, and the physical meanings of the theories presented. The assumptions and the approximations made in the formulations are explicitly stated, and their limitations and extensions are discussed. Comparisons with exact analytical solutions and rigorous numerical simulations are made to support the arguments. Issues that were debated in the literature will be commented on and discussed when they are related to the logical development.

The paper is organized as follows: a brief historical review is given in Section 2, in which the key issues that arose in the late 1980's are presented and discussed. The coupled-mode formulations for uniform, grating-assisted, and tapered couplers are discussed in Sections 3, 4, and 5, respectively. Each section starts with a brief description of the conventional CMT and its applications. The

0740-3232/94/030963-21$06.00 

nonorthogonal coupled-mode equations are derived, and their distinct features are described. The solutions of the coupled-mode equations are then presented, and comparisons with the solutions of conventional CMT, the exact analytical solutions, and the numerical simulations are made. A brief conclusion is given in Section 6.

## 2. BRIEF HISTORICAL REVIEW

The heuristic coupled-mode theory was first developed by Pierce[9] and Miller[10] in the early 1950's. The rigorous formulations of the coupled-mode equations were later established by Schelkunoff[11] and Haus,[12] who used a mode expansion and a variational principle, respectively. The initial applications of the CMT were to microwave oscillation and propagation. The CMT was introduced to guided-wave optics by Snyder,[13] Marcuse,[14] Yariv,[15] and Kogelnik[16] in the early 1970's. The CMT was used to analyze mode coupling or conversion in optical waveguides.[3] It was also used to explore novel optical guided-wave devices.[2-6] Examples of the latter category are distributed feedback lasers[17] and $\Delta\beta$ coupler switches,[18] both invented by Herwig Kogelnik and his co-workers at Bell Laboratories. The coupled-mode theory has also been very useful in our understanding of nonlinear optical wave propagation and interaction, such as second harmonic generation, parametric amplification, and modulation instability.[7,8]

One of the basic elements used as a building block for a range of optical guided-wave devices is the system of coupled waveguides. The physical models for coupled-waveguide systems consist of two or more dielectric waveguides placed in close proximity. These waveguides may be parallel to each other or may have variable separations. They may be subject to index perturbations such as gratings, tapers, nonlinearities, and loss or gain along the waveguide axes. The index perturbations may be caused by imperfections in material processing and device fabrication; in some cases their effects may be undesirable and should be assessed and minimized. In many cases, however, the index perturbations are created on purpose for reflecting, switching, and modulating the light in the waveguides.

The analysis of the coupled-waveguide systems by the conventional CMT was based almost exclusively on the modes of the individual, or uncoupled, waveguides. Once these waveguide modes, i.e., their propagation constants and field patterns, are determined, the amplitudes of the modes in the coupled-waveguide systems are governed by the coupled-mode equations. The solutions of the coupled-mode equations describe wave propagation and coupling in the coupled-waveguide system. Together with the field distribution over the transverse cross section, the coupled-mode analysis provides a simple and intuitive yet rigorous description of electromagnetic wave propagation and interaction in a coupled-waveguide system.

A number of approximations are assumed in the formulations and often in the solutions of the coupled-mode equations. One of the assumptions for the conventional CMT is that the waveguide modes are orthogonal to each other. This approximation was considered to be acceptable and was taken for granted until Hardy and Streifer[19] in 1986 suggested a modified coupled-mode formulation in which nonorthogonality was considered. This new nonorthogonal CMT was shown to yield more-accurate dispersion curves and field patterns for the composite modes (or normal modes) of the parallel coupled waveguides. In their original paper, Hardy and Streifer did not establish the self-consistency of their formulations by demonstrating the power conservation for a lossless system. The self-consistent nonorthogonal coupled-mode formulations for the parallel coupled-waveguide systems were developed later by Haus and coworkers, who used a variational principle[20]; by Chuang, who used the reciprocity theorem[21]; and also by Hardy and Streifer in Ref. 22 through reformulation. There are some minor discrepancies among the various formulations advanced by different groups.[20-22] These differences were examined by Vassello[23] and were shown to be subtle theoretically but of little practical significance.

In the course of the development, criticism was raised by Snyder and co-workers about the validity and accuracy of the new nonorthogonal CMT. In a series of papers[24,25] they showed that the nonorthogonal formulations can lead to erroneous results for the coupling length of the TM modes of parallel slabs when the index discontinuity is large. Furthermore, they demonstrated that the conventional orthogonal coupled-mode theory that is based on the same waveguide modes predicts the coupling length well for the case of a large index difference. This finding was somewhat unexpected. In both the nonorthogonal and the conventional orthogonal coupled-mode formulations, the same trial solution, i.e., the linear superposition of the waveguide modes, is utilized. It appears that the nonorthogonal CMT contains fewer approximations and should be more accurate than the conventional one, which, as a matter of fact, can be derived from the former under certain conditions. This paradox puzzled many researchers and triggered a series of debates.[24-35]

There were, as a matter of fact, two issues involved in the arguments that were often confused and misinterpreted. The first issue is related to the cross power, the second one to the polarization effect. Since the cross-power terms, or overlap integrals, appear naturally in the derivation of the CMT as a result of the inherent modal nonorthogonality, the question is whether it is necessary, worthwhile, or even legitimate to retain them. To make our discussion easier, let us examine the scalar CMT, in which the field is represented by a summation of the scalar modes of the individual waveguides.[36-41] For a coupler made of identical waveguides, the effective indices of the symmetric and the antisymmetric normal modes can be approximated by[38,40,41]

$$N_s = N_{\text{eff}} + \frac{k_{11} - Xk_{12}}{1 - X^2} + \frac{k_{12} - Xk_{11}}{1 - X^2}, \tag{2.1a}$$

$$N_a = N_{\text{eff}} + \frac{k_{11} - Xk_{12}}{1 - X^2} - \frac{k_{12} - Xk_{11}}{1 - X^2}, \tag{2.1b}$$

where $N_{\text{eff}}$ is the effective index of the individual guide and $X$ is the cross power. $k_{ij}$ are the normalized coupling coefficients and may be expressed by

$$k_{ij} = \frac{1}{4}\sqrt{\frac{\epsilon_0}{\mu_0}}\int (n^2 - n_j^2)\Psi_i^*\Psi_j \mathrm{d}a. \tag{2.2}$$

By use of a perturbation analysis and treatment of $\exp(-\alpha S)$ as the small parameter ($\alpha$ is the transverse decay constant and $S$ is half of the separation between the two guides), it is shown that a first-order approximation yields[24,25,38]

$$N_s = N_{\text{eff}} + k_{12}, \tag{2.3a}$$

$$N_a = N_{\text{eff}} - k_{12}, \tag{2.3b}$$

which is the result of the conventional CMT. Although this analysis is legitimate, the first-order results in Eqs. (2.3) are reliable only when the refractive-index difference is not too small and the two waveguides are sufficiently far apart. In fact, when the index difference is small and the two guides are close to each other, the cross power $X$ is much larger than the normalized coupling coefficient $k_{12}$ that is proportional to the index difference weighted by the overlap integral. Under this circumstance, one should retain the cross power [or, more precisely, $Xk_{12}$ in Eqs. (2.1)] to obtain accurate effective indices. This conclusion is valid for the TE modes of slab waveguides, as well, and is supported by examples in Refs. 19–23, 26, 27, and 29 (see also Subsections 3.C and 3.D below).

On the other hand, the parameter describing the physics of the power transfer between waveguides is the beat length, which is related to the difference between the effective indices, i.e.,

$$L_c = \frac{\lambda}{2(N_s - N_a)}, \tag{2.4}$$

where $\lambda$ is the wavelength. By using Eqs. (2.1), (2.2), and (2.4), one readily derives

$$L_c = \frac{1 - X^2}{k_{12} - Xk_{11}} \frac{\lambda}{4} \tag{2.5}$$

from the nonorthogonal CMT. If the cross power $X$ can be neglected, then the coupling length reduces to

$$L_c = \frac{1}{k_{12}} \frac{\lambda}{4}, \tag{2.6}$$

which is the result obtained by the conventional coupled-mode formulation. By inspection of Eq. (2.5), one notes that the first two terms in Eqs. (2.1) are canceled and that they made no contribution to $L_c$. Hence the effect that is due to $Xk_{12}$ is absent in the determination of the coupling length. The higher-order terms $X^2$ and $Xk_{11}$ have little effect, and hence Eq. (2.6) is highly accurate (see the discussion in Subsection 3.E below).

If the two waveguides are dissimilar, then the conventional coupled-mode formulation is not self-consistent, as pointed out by Hardy and Streifer.[19] The expressions for the coupling coefficients indicate that $k_{12} \neq k_{21}$. This is contradictory to the power conservation of the conventional CMT, which requires that $k_{12} = k_{21}$. Under this circumstance, the cross-power term is necessary for the self-consistency of the CMT. To develop a self-consistent orthogonal CMT based on the waveguide modes, the coupling coefficients should be redefined as shown in Section 3.D below.

Therefore, under the scalar approximation and for synchronized waveguides, the nonorthogonal CMT is necessary for accurate effective indices of the normal modes when the two waveguides are strongly coupled. On the other hand, the coupling length, and therefore the power exchange between the waveguides, may be accurately described by the conventional orthogonal coupled-mode theory, and the more complicated nonorthogonal CMT may not be necessary for weakly coupled waveguides. For dissimilar waveguides the conventional CMT is not self-consistent, and the nonorthogonal CMT is necessary. A self-consistent orthogonal CMT may be established by a new definition of the coupling coefficients. It should be emphasized that the linear combination of the individual waveguide modes, on which both the conventional and the improved CMT's are based, is only an approximation to the exact fields in the coupled waveguides. Strictly speaking, both formulations are valid only for weakly coupled waveguides, although the improved CMT is indeed more accurate for weakly guiding waveguides under scalar approximation.

For the vector formalisms in which the fields are represented by a summation of the vector modes of the individual waveguides, there is some inherent inconsistency in the trial solution itself, independent of the cross-power issue. This fundamental error was pointed out by Snyder and co-workers[24,25,28,33] and was examined further by Haus *et al.*[35] Generally speaking, the trial solutions do not satisfy the boundary conditions for the electric fields. When the index discontinuities are weak, this approximation is acceptable and the coupled-mode theory that is based on such trial solutions is reliable. Under this condition the nonorthogonal CMT is more accurate than the conventional one, especially when the two waveguides are closely coupled. This situation is similar to the scalar case and is evidenced in the examples shown in Refs. 24–35. When the index discontinuities are large, the errors in the trial solutions will become more pronounced. Since the same trial solutions are assumed in both the conventional and the improved CMT's, one expects that neither will be reliable in the treatment of the polarization effect in strongly guided structures. The puzzling fact is that Snyder and co-workers demonstrated that the conventional CMT yields very accurate coupling lengths for the TM modes of the coupled slabs even when the index difference is large, whereas the nonorthogonal CMT gives erroneous results. This phenomenon is explained in Refs. 33 and 35. It was found that the errors in the trial solutions do not affect the coupling coefficient $k_{12}$ but have much more significant effects on $k_{11}$ and, to some extent, on $X$ also. Consequently, the coupling length predicted by Eq. (2.6) from the conventional CMT is more reliable than that calculated by Eq. (2.5) from the nonorthogonal CMT. However, this does not lead to the conclusion that the conventional CMT is reliable for strongly guiding structures. As far as the propagation constants and the field patterns are concerned, neither the conventional nor the improved CMT's are reliable, and more-accurate trial solutions are needed. More discussion about the issue of improved trial solutions is presented in Subsection 3.F below.

Despite the controversies the nonorthogonal CMT attracted much attention and was applied to a range of optical guided-wave devices that were based on coupled-waveguide structures. Simplified scalar versions were devised.[36–41] Formulations for multiwaveguide and multi-

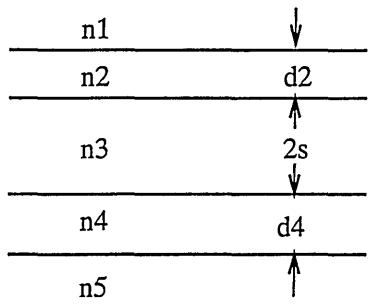


Fig. 1. Schematic diagram of a uniform directional coupler.

mode structures,[42–47] anisotropic media,[48,49] periodic grating structures,[50–58] tapered structures,[59–66] and nonlinear couplers[67] were developed. Applications to various directional couplers in integrated and fiber optics[68–80] were carried out. Some experimental work by Marcatili *et al.*[81] and by Syms and Peall[82] was also published, and their findings appeared to support the merit of the nonorthogonal CMT.

## 3. COUPLED-MODE THEORY FOR UNIFORM COUPLERS

The simplest model for the coupled-waveguide system is a directional coupler consisting of two uniform, parallel waveguides in close proximity (Fig. 1). The transverse cross sections of the waveguides are assumed to be arbitrary. If the waveguides are made of multiple layers of step-index profile, one can obtain exact solutions to the modal problem by using the transfer-matrix method.[6] For most of the practical directional couplers made of channel waveguides or circular fibers, however, exact analytical solutions are difficult to find. One may resort to more-sophisticated numerical techniques for rigorous solutions, but such approaches are more computation intensive and less intuitive. The coupled-mode theory is extremely useful in providing simple analytical solutions that give insight into the mode-coupling process in directional coupler devices.

### A. Conventional Coupled-Mode Theory

The conventional coupled-mode theory can be derived in a simple, intuitive way. Consider guided modes in the individual waveguides, with the implicit time dependence $\exp(j\omega t)$. Denote the amplitudes of these modes by $a_1$ and $a_2$. When the two waveguides are infinitely far apart the mode amplitudes will obey the equations

$$\frac{da_1}{dz} = -j\beta_1 a_1, \tag{3.1a}$$

$$\frac{da_2}{dz} = -j\beta_2 a_2. \tag{3.1b}$$

Hence these waveguide modes will propagate independently with their propagation constants $\beta_1$ and $\beta_2$.

When the two waveguides are brought into close proximity, the modes will couple to each other as a result of the interaction of the evanescent fields. Mathematically, the spatial dependences of one mode amplitude will be modified by the existence of the other. If the coupling is weak, then the coupled equations should be of the form

$$\frac{da_1}{dz} = -j(\beta_1 + K_{11})a_1 - jK_{12}a_2, \tag{3.2a}$$

$$\frac{da_2}{dz} = -j(\beta_2 + K_{22})a_2 - jK_{21}a_1, \tag{3.2b}$$

where $K_{12}$, $K_{21}$, and $K_{11}$, $K_{22}$ are the mutual and the self-coupling coefficients, respectively.

Furthermore, if the coupled-waveguide system is lossless, then self-consistency requires that Eqs. (3.2) satisfy the law of power conservation. Assume that the two waveguide modes are power orthogonal. The total guided power can be written as

$$P(z) = |a_1|^2 + |a_2|^2. \tag{3.3}$$

Note that we have normalized the mode amplitudes $a_1$ and $a_2$ so that their squares are equal to the powers in the modes. The law of power conservation requires that

$$\frac{d}{dz}P(z) = 0. \tag{3.4}$$

Because Eq. (3.4) is independent of the initial condition, the coupling coefficients obey the following relations:

$$K_{12} = K_{21}^* = \kappa, \tag{3.5}$$

and $K_{11}, K_{22}$ have to be real.

For the uniform couplers, both the propagation constants and the coupling coefficients are independent of $z$, and therefore Eqs. (3.2) can be solved analytically. For the sake of simplicity, we may take out a common phase factor in the mode amplitudes by letting

$$a_i(z) = \hat{a}_i \exp\left(-j\frac{\beta_1 + K_{11} + \beta_2 + K_{22}}{2}z\right). \tag{3.6}$$

Equations (3.2) are recast into

$$\frac{d\hat{a}_1}{dz} = -j\delta\hat{a}_1 - j\kappa\hat{a}_2, \tag{3.7a}$$

$$\frac{d\hat{a}_2}{dz} = +j\delta\hat{a}_2 - j\kappa\hat{a}_1, \tag{3.7b}$$

where

$$\delta = \frac{\beta_1 + K_{11} - \beta_2 - K_{22}}{2} \tag{3.8}$$

is the detuning or phase-mismatch factor. One may rewrite Eqs. (3.7) in a compact matrix form:

$$\frac{d}{dz}\mathbf{A} = -j\overline{\mathbf{H}}\mathbf{A}, \tag{3.9}$$

where

$$\mathbf{A} = \begin{bmatrix} \hat{a}_1 \\ \hat{a}_2 \end{bmatrix}, \tag{3.10}$$

$$\overline{\mathbf{H}} = \begin{bmatrix} +\delta & \kappa \\ \kappa & -\delta \end{bmatrix}. \tag{3.11}$$

Since $\overline{\mathbf{H}}$ is Hermitian for a lossless system, it can be diagonalized by a unitary matrix such that

$$\mathbf{O}^t\overline{\mathbf{H}}\mathbf{O} = \mathbf{B}, \tag{3.12}$$

where $\mathbf{B}$ is a diagonal matrix,

$$\mathbf{B} = \begin{bmatrix} \beta_s & 0 \\ 0 & \beta_a \end{bmatrix}, \tag{3.13}$$

and

$$\mathbf{O} = \begin{bmatrix} \cos(\eta/2) & -\sin(\eta/2) \\ \sin(\eta/2) & \cos(\eta/2) \end{bmatrix}, \tag{3.14}$$

where the parameter $\eta$ is defined by

$$\tan(\eta) = \frac{\kappa}{\delta}. \tag{3.15}$$

The diagonal elements $\beta_s$ and $\beta_a$ are the propagation constants of the normal modes of the parallel coupler (i.e., the composite modes). To see this, one can make the transformation

$$\mathbf{A} = \mathbf{O}\mathbf{W}, \tag{3.16}$$

under which the coupled-mode equation (3.9) reduces to

$$\frac{\mathrm{d}}{\mathrm{d}z}\mathbf{W} = -j\mathbf{B}\mathbf{W}. \tag{3.17}$$

There is no coupling between the two modes in Eq. (3.17). Hence $\mathbf{W}$ may be interpreted as the amplitude matrix for the normal modes of the parallel waveguides with propagation constants $\beta_s$ and $\beta_a$, representing the symmetric-like and antisymmetriclike composite modes, respectively. Equation (3.17) can be readily integrated. The mode amplitudes may be expressed in terms of the transfer matrix as

$$\mathbf{A}(z) = \mathbf{T}(z)\mathbf{A}(0), \tag{3.18}$$

where

$$\mathbf{T} = \mathbf{O}\begin{bmatrix} \exp(-j\beta_s z) & 0 \\ 0 & \exp(-j\beta_a z) \end{bmatrix}\mathbf{O}^{-1}, \tag{3.19}$$

or more explicitly, the matrix elements can be given by

$$t_{11} = t_{22}^* = \cos(Sz) - j\cos(\eta)\sin(Sz), \tag{3.20a}$$

$$t_{12} = t_{21} = -j\sin(\eta)\sin(Sz), \tag{3.20b}$$

where

$$S \doteq \sqrt{\delta^2 + \kappa^2}. \tag{3.21}$$

The propagation constants of the composite modes are

$$\beta_s = \beta_0 + S, \tag{3.22a}$$

$$\beta_a = \beta_0 - S, \tag{3.22b}$$

where

$$\beta_0 = \frac{\beta_1 + K_{11} + \beta_2 + K_{22}}{2}. \tag{3.23}$$

Suppose that, at the input, only one waveguide is excited, i.e., $a_1(0) = 1$ and $a_2(0) = 0$. The guided powers in waveguides 1 and 2 can be given by

$$P_1(z) = \cos^2(Sz) + \cos^2(\eta)\sin^2(Sz), \tag{3.24a}$$

$$P_2(z) = \sin^2(\eta)\sin^2(Sz). \tag{3.24b}$$

Maximum power transfer from guide 1 to guide 2 occurs at $z = L_c$, where

$$L_c = \pi/(2S), \tag{3.25}$$

and is equal to

$$P_2|_{\max} = \sin^2(\eta). \tag{3.26}$$

It is noted that, for complete power transfer, the two waveguide modes have to be phase matched, i.e., $\delta = 0$. According to the conventional CMT there is no cross talk at the coupling length defined by Eq. (3.25). Consequently the power-extinction ratio, defined as

$$\text{E.R.} = \frac{P_1|_{\min}}{P_2|_{\max}}, \tag{3.27}$$

is identically zero.

### B. Nonorthogonal Coupled-Mode Equations

The conventional CMT for the coupled-waveguide systems is set up in a simple and intuitive way. The formulations are general and are expected to be valid under the weak-coupling and the power-orthogonal assumptions. For evaluation and assessment of these assumptions in the heuristic coupled-mode formulation, a more rigorous and systematic approach is necessary.

A unique feature associated with uniform (or $z$-invariant) waveguide structure is that a variational (or, more precisely, stationary) expression for the propagation constant of the normal mode of the coupled system can serve as a formal mathematical basis for the coupled-mode equations.[20] We may use either the vector[19-23] or the scalar[36-41] modes as trial solutions to derive the coupled-mode equations. The more rigorous vector modes are chosen for this paper, although the scalar modes may be sufficient for many applications. In addition, it is supposed that each waveguide in isolation supports only one guided mode. To treat multimode waveguides or to account for the radiation modes is possible[46-48,62] but would be more complicated and tedious. The trial solution may be expressed in terms of a linear superposition of the waveguide modes:

$$\mathbf{E} = a_1(z)\mathbf{e}_1 + a_2(z)\mathbf{e}_2, \tag{3.28a}$$

$$\mathbf{H} = a_1(z)\mathbf{h}_1 + a_2(z)\mathbf{h}_2, \tag{3.28b}$$

where $\mathbf{e}_i$ and $\mathbf{h}_i$ are the vector waveguide modes and $a_1$ and $a_2$ are the corresponding mode amplitudes.

The trial solution assumed in Eqs. (3.28) is only an approximation to the electromagnetic fields in the coupled-waveguide systems. The degree of accuracy and the scope of validity of this approximation are yet to be verified. Nevertheless, the stationary property of the variational expression ensures that errors in the propagation constants are not sensitive to the errors made in the trial solution in Eqs. (3.28).[20] For this reason the propagation constants that one obtains by solving the coupled-mode equations are expected to be of greater accuracy than the trial solutions.

By substituting Eqs. (3.28) into the variational expression and utilizing the stationary property,[20] one may obtain, for the coupled-mode equations,

$$\sum_j P_{ij}\frac{da_j}{dz} = j\sum_j \overline{H}_{ij}a_j, \tag{3.29}$$

where

$$\overline{H}_{ij} = P_{ij}\beta_j + \overline{K}_{ij}, \tag{3.30}$$

$$P_{ij} = \frac{1}{4}\int [\mathbf{e}_i^* \times \mathbf{h}_j + \mathbf{e}_j \times \mathbf{h}_i^*] \cdot \hat{z}\,da \tag{3.31}$$

are the power marix elements and

$$\overline{K}_{ij} = \frac{1}{4}\omega\epsilon_0\int (\overline{n}^2 - n_j^2)\mathbf{e}_i^* \cdot \mathbf{e}_j\,da \tag{3.32}$$

are the coupling coefficients for the natural coupling between the two waveguides; $\overline{n}$ is the actual refractive-index distribution of the coupler, and $n_i(x, y)$ is the index of the $i$th guide in the absence of the other waveguides. The derivation indicates that the coupled-mode equations result from an optimization by the application of a variational principle. In this sense the solutions to the coupled-mode equations represent the best-possible solutions to the coupled-waveguide systems that are based on the trial solutions used. In the above derivation the waveguide systems are assumed to be lossless. A similar approach may be applied to the lossy waveguides with some modifications to the cross power and the coupling coefficients.[21]

For a lossless system the law of power conservation implies that

$$\frac{d}{dz}\sum a_i^* P_{ij} a_j = 0. \tag{3.33}$$

It follows from Eq. (3.29) that

$$\overline{H}_{ij} = \overline{H}_{ji}^* \tag{3.34a}$$

or

$$P_{ij}(\beta_j - \beta_i) = \overline{K}_{ij} - \overline{K}_{ji}^*. \tag{3.34b}$$

We note that, unless $\beta_i = \beta_j$, $\overline{K}_{ij}$ is not equal to $\overline{K}_{ji}^*$. This is in contrast to the conventional coupled-mode formulation, which states that the coupling coefficients are symmetrical for the lossless systems, regardless of the difference between the $\beta_i$. Figure 2 shows $(\overline{K}_{12} - \overline{K}_{21}^*)/K$ in percentage as a function of the separation $2S$ between the two slabs. The parameter $K$ is the average of the two coupling coefficients; i.e., $K = (\overline{K}_{12} + \overline{K}_{21}^*)/2$. The indices of the waveguides are $n_1 = n_3 = n_5 = 3.200$ and $n_2 = 3.250$. The index of the other guiding layer, $n_4$, is varied as $\delta n = n_2 - n_4 = 0.01$, 0.1, and 0.2. The widths of the two slabs are $d_2 = d_4 = 1.0$ $\mu$m. The wavelength is $\lambda = 1.5$ $\mu$m. The results indicate that $\overline{K}_{12}$ is nearly equal to $\overline{K}_{21}$ when the two waveguides are very similar. But the difference between $\overline{K}$ and $\overline{K}$ can be as large as 100% as the degree of the asymmetry increases. We also note that the percentage difference does not vanish as the two waveguides become large. In this sense there is an inherent inconsistency in the conventional coupled-mode theory that is based on the individual waveguide modes when it is applied to the couplers made of dissimilar waveguides. This fact was first pointed out by Hardy and Streifer[19] and was subsequently demonstrated by others.[20,21]

### C. Solutions to the Coupled-Mode Equations

Assume the normalization of Eq. (3.31) to be $P_{11} = P_{22} = 1$, and let $P_{12} = P_{21} = X$. We may recast the coupled-mode equations in a compact matrix form:

$$\mathbf{P}\frac{d}{dz}\mathbf{A} = -j\overline{\mathbf{H}}\mathbf{A}, \tag{3.35}$$

where

$$\mathbf{P} = \begin{bmatrix} 1 & X \\ X & 1 \end{bmatrix}. \tag{3.36}$$

Since $\mathbf{P}$ is positive definite and $\overline{\mathbf{H}}$ is Hermitian, these two matrices can be diagonalized simultaneously by a transformation matrix $\mathbf{O}$ such that

$$\mathbf{O}^t\mathbf{P}\mathbf{O} = \mathbf{I}, \tag{3.37a}$$

$$\mathbf{O}^t\overline{\mathbf{H}}\mathbf{O} = \mathbf{B}, \tag{3.37b}$$

where $\mathbf{I}$ is the identity matrix and $\mathbf{B}$ is a diagonal matrix for the propagation constants of the composite modes. The subscript $t$ stands for the transpose of the matrix. $\mathbf{O}$ can be written as

$$\mathbf{O} = \frac{1}{\cos(\alpha)}\begin{bmatrix} \cos\left(\frac{\eta+\alpha}{2}\right) & -\sin\left(\frac{\eta+\alpha}{2}\right) \\ \sin\left(\frac{\eta-\alpha}{2}\right) & \cos\left(\frac{\eta-\alpha}{2}\right) \end{bmatrix}, \tag{3.38}$$

where the parameter $\alpha$ is related to the cross power as

$$\sin(\alpha) = X \tag{3.39}$$

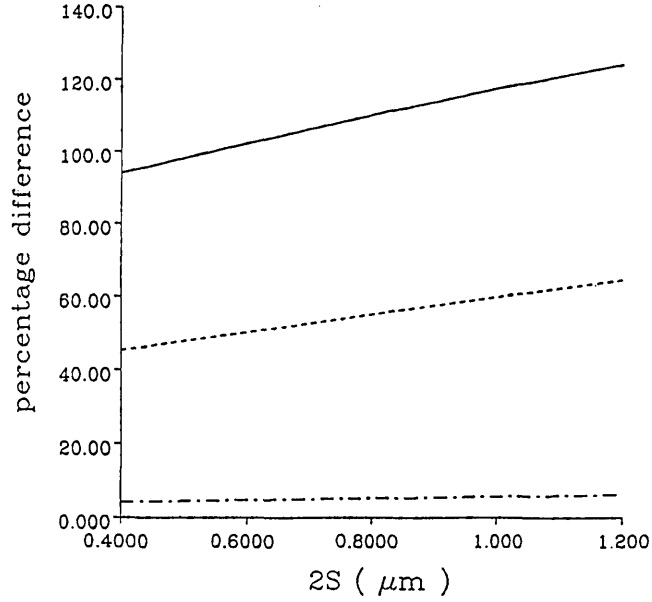


Fig. 2. Percentage difference between the coupling coefficients $(\overline{K}_{12} - \overline{K}_{21}^*)/2(\overline{K}_{12} + \overline{K}_{21}^*)$ as a function of the separation for TE modes of an asymmetric slab coupler. $n_1 = n_3 = n_5 = 3.200$ and $n_2 = 3.250$. The index $n_4$ varies as $\delta n = n_2 - n_4 = 0.01, 0.1, 0.2$. The widths of the two slabs are $d_2 = d_4 \times 1.0$ $\mu$m. The wavelength is $\lambda = 1.5$ $\mu$m.

and $\eta$ is defined by an equation that is the same as Eq. (3.15) except that the effective coupling coefficient is redefined as

$$\kappa = \frac{\overline{K}_{12} + \overline{K}_{21} - X(\overline{K}_{11} + \overline{K}_{22})}{2(1 - X^2)^{1/2}}. \tag{3.40}$$

The transfer matrix $\mathbf{T}(z)$ is calculated with Eqs. (3.19) and (3.38) and is found to be

$$t_{11} = t_{22}^* = \frac{\cos(\alpha)\cos(Sz) - j\cos(\eta)\sin(Sz)}{\cos(\alpha)}, \tag{3.41a}$$

$$t_{12} = -j\frac{\sin(\eta + \alpha)\sin(Sz)}{\cos(\alpha)}, \tag{3.41b}$$

$$t_{21} = -j\frac{\sin(\eta - \alpha)\sin(Sz)}{\cos(\alpha)}, \tag{3.41c}$$

where $S$ is defined by Eq. (3.21), with $\kappa$ given by Eq. (3.40).

The propagation constants of the composite modes are given by formulas that are the same as Eqs. (3.22) except that $\beta_0$ is expressed by

$$\beta_0 = \frac{\beta_1 + \beta_2}{2} + \frac{\overline{K}_{11} + \overline{K}_{22} - X(\overline{K}_{12} + \overline{K}_{21})}{2(1 - X^2)} \tag{3.42}$$

and $\kappa$ is replaced by Eq. (3.40). The field patterns are derived from Eqs. (3.16), (3.28), and (3.38):

$$\mathbf{e}_s = \frac{\cos[(\eta + \alpha)/2]}{\cos(\alpha)}\mathbf{e}_1 + \frac{\sin[(\eta - \alpha)/2]}{\cos(\alpha)}\mathbf{e}_2, \tag{3.43a}$$

$$\mathbf{e}_a = -\frac{\sin[(\eta + \alpha)/2]}{\cos(\alpha)}\mathbf{e}_1 + \frac{\cos[(\eta - \alpha)/2]}{\cos(\alpha)}\mathbf{e}_2. \tag{3.43b}$$

### D. Self-Consistent Orthogonal Coupled-Mode Theory

In comparison with the conventional orthogonal coupled-mode theory presented in Subsection 3.A, the new entity in the nonorthogonal coupled-mode formulation is the overlap integral $X$. If $X$ is small and neglected, then the solutions derived in Subsection 3.C are reduced formally to those of the conventional theory in Section 3.A, with the coupling coefficients redefined as

$$\kappa = \frac{\overline{K}_{12} + \overline{K}_{21}}{2}. \tag{3.44}$$

Therefore a self-consistent orthogonal coupled-mode formulation may be established by modification of the coupling coefficients in the conventional coupled-mode equations. The propagation constants of the composite modes are

$$\beta_s = \frac{\beta_1 + \beta_2 + \overline{K}_{11} + \overline{K}_{22}}{2} + \left[\delta^2 + \left(\frac{\overline{K}_{12} + \overline{K}_{21}}{2}\right)^2\right]^{1/2}, \tag{3.45a}$$

$$\beta_a = \frac{\beta_1 + \beta_2 + \overline{K}_{11} + \overline{K}_{22}}{2} - \left[\delta^2 + \left(\frac{\overline{K}_{12} + \overline{K}_{21}}{2}\right)^2\right]^{1/2}, \tag{3.45b}$$

and the field patterns are

$$\mathbf{e}_s = \cos(\eta/2)\mathbf{e}_1 + \sin(\eta/2)\mathbf{e}_2, \tag{3.46a}$$

$$\mathbf{e}_a = -\sin(\eta/2)\mathbf{e}_1 + \cos(\eta/2)\mathbf{e}_2. \tag{3.46b}$$

To assess the accuracy of the coupled-mode formulations established above, my colleagues and I calculated both the propagation constants and the field patterns of the composite modes of a parallel directional coupler. The parameters are the same as those used in Fig. 2, except that the refractive indices $n_2$ are chosen to be 3.25 and 3.23 for the cases of identical and dissimilar waveguides, respectively. Figure 3 displays the effective indices of the TE composite modes. It is demonstrated that the nonorthogonal CMT (dashed curves) yields dispersion curves in closer agreement with the exact solutions (solid curves) than does the self-consistent orthogonal theory (dashed–dotted curves), in particular when the two waveguides are

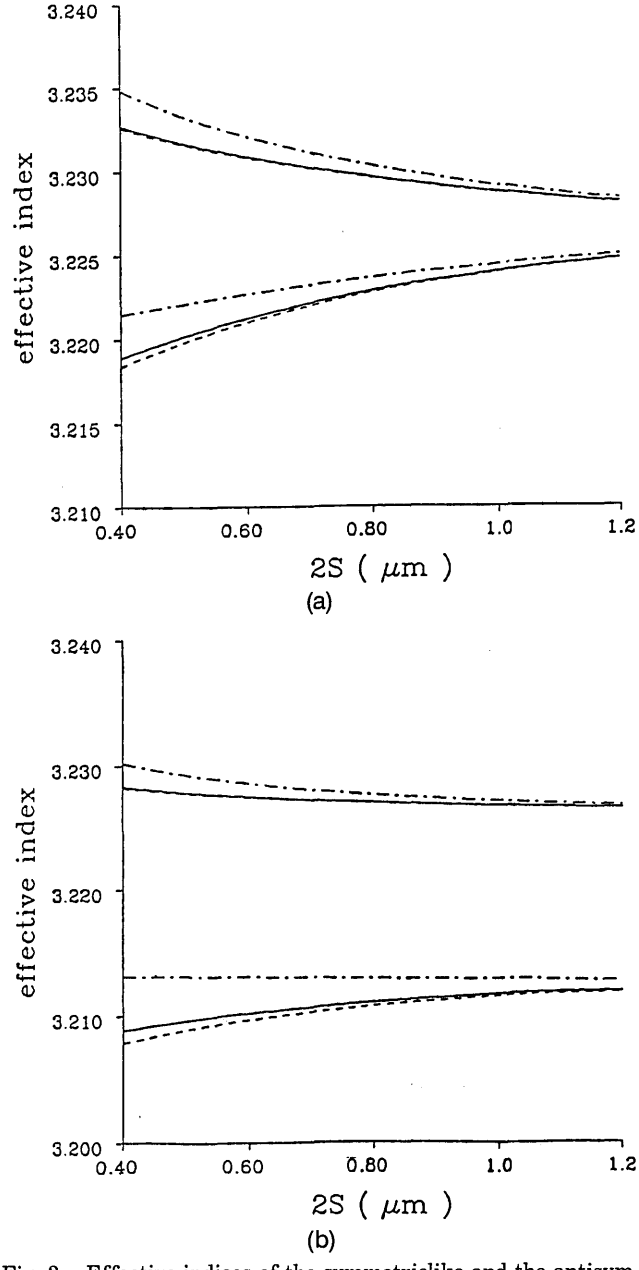


Fig. 3. Effective indices of the symmetriclike and the antisymmetriclike composite modes of the uniform directional couplers: (a) identical waveguides, (b) dissimilar waveguides. Solid curves, exact solutions; dashed curves, nonorthogonal CMT; dashed–dotted curves, orthogonal CMT. The parameters are the same as those in Fig. 2 except that (a) $n_2 = 3.25$ and (b) $n_2 = 3.23$.

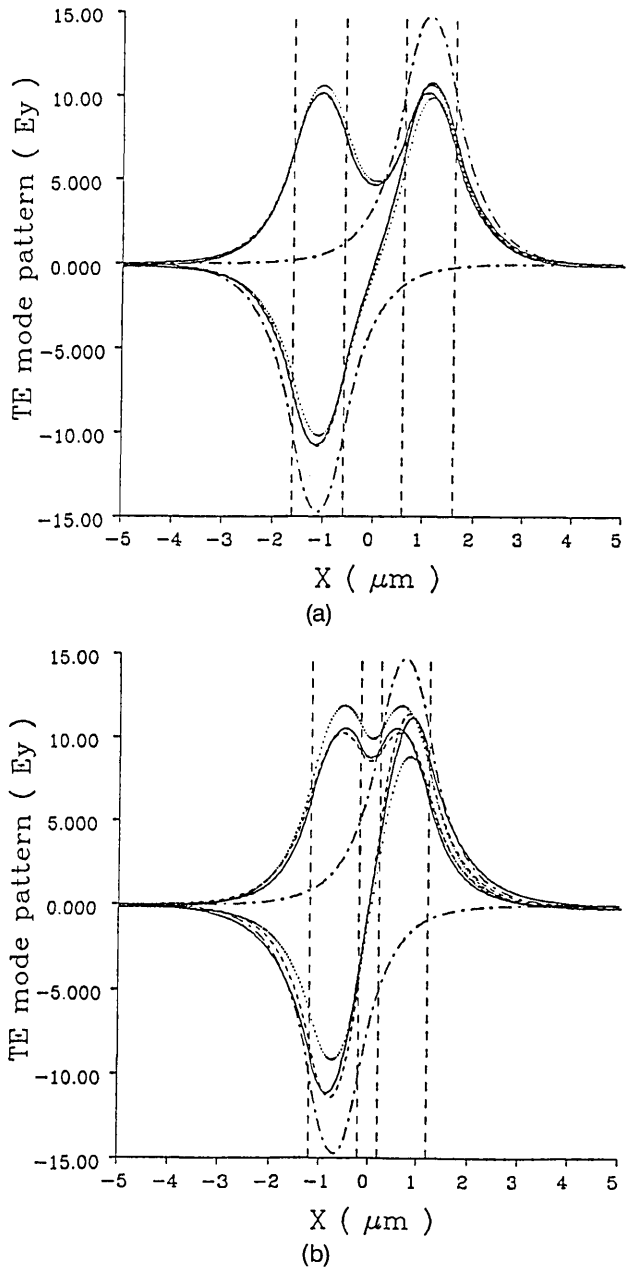


Fig. 4. Electric-field patterns of the symmetriclike and the antisymmetriclike composite modes of the uniform directional couplers made of identical waveguides shown in Fig. 3 (a). Solid curves, exact solutions; dashed curves, nonorthogonal CMT; dotted curves, orthogonal CMT; dashed–dotted curves, waveguide modes. (a) $2S = 1.0$ $\mu$m, (b) $2S = 0.2$ $\mu$m.

closely coupled. The electric-field patterns for the composite modes are shown in Figs. 4 and 5. The separations between the slabs are assumed to be $2S = 1.0$ and 0.2 $\mu$m, representing a weak and a strong coupled waveguide system, respectively. In comparison with the exact solutions (solid curves), the nonorthogonal CMT (dashed curves) is indeed superior to the orthogonal CMT (dotted curves) for the field patterns, too. As a matter of interest, the field patterns of the waveguide modes (dashed–dotted curves also were plotted). The waveguide modes become acceptable approximations of the exact composite modes only when the two waveguides are weakly coupled and far from synchronism.

### E. Power Coupling between Waveguides

The most important function of the directional coupler is to couple power from one guide to another. The total power guided in the entire coupled-waveguide system is defined, as usual, as

$$P(z) = \frac{1}{4}\int (\mathbf{E} \times \mathbf{H}^* + \mathbf{E}^* \times \mathbf{H}) \cdot \hat{z}\,da = \sum_{ij} a_i^*(z) P_{ij} a_i(z). \tag{3.47}$$

Because of the nonorthogonality, the total guided power is related not only to the magnitudes of the mode amplitudes $|a_i(z)|^2$ but also to the cross product of different mode amplitudes through the overlap integrals (the cross power).

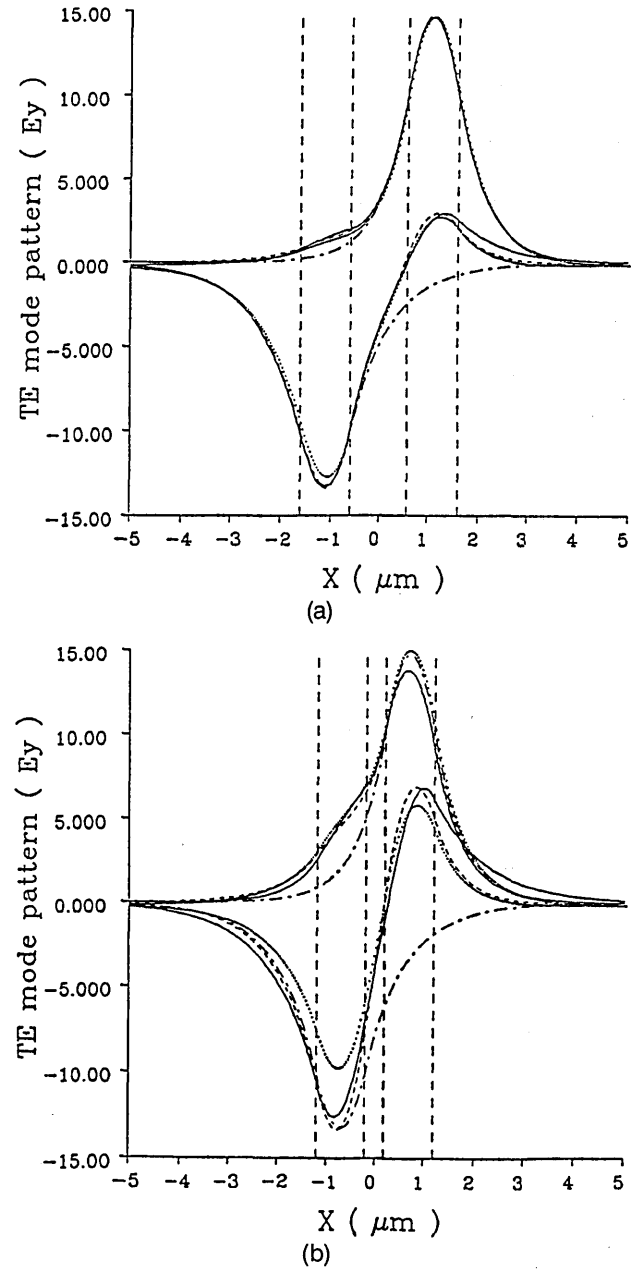


Fig. 5. Electric-field patterns of the symmetriclike and the antisymmetriclike composite modes of the uniform directional couplers made of dissimilar waveguides shown in Fig. 3(a). Solid curves, exact solutions; dashed curves, nonorthogonal CMT; dotted curves, orthogonal CMT; dashed–dotted curves, waveguide modes. (a) $2S = 1.0$ $\mu$m; (b) $2S = 0.2$ $\mu$m.

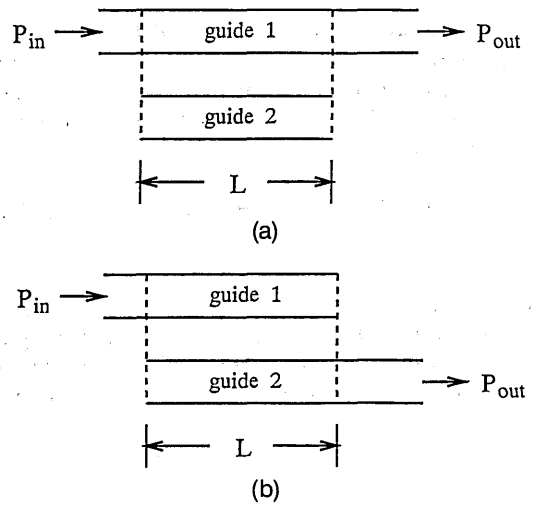


Fig. 6. Input and output structures assumed for the guided power in an individual waveguide: (a) Guided power in waveguide 1, (b) guided power in waveguide 2.

To define the guided power in an individual waveguide in the coupled systems is somewhat tricky. Conceptually, to measure the power in a single waveguide along $z$, one should terminate the other waveguide so that the power will be guided out through the waveguide of interest. Two such configurations are depicted in Fig. 6. Application of a simple mode-matching method[83] yields the amplitude of the guided mode in the $i$th waveguide, expressed by

$$b_i(z) = a_i(z) + Xa_j(z), \tag{3.48}$$

and the guided power in that waveguide is

$$P_i(z) = |b_i(z)|^2 = |a_i(z) + Xa_j(z)|^2. \tag{3.49}$$

According to Eq. (3.49), not only the mode amplitude $a_i$ but also the mode in the other waveguide $a_j$ will contribute to the guided power in waveguide $i$, a conclusion different from that predicted by the conventional CMT. Suppose that, at the input, only guide 1 is excited, i.e., $a_1(0) = 1$ and $a_2(0) = 0$. The mode amplitudes at an arbitrary position along $z$ can be determined by the transfer matrix in Eq. (3.38). The output powers from guides 1 and 2, respectively, are given by

$$P_1(z) = \cos^2(Sz) + \left[\frac{\cos(\eta) - \sin(\alpha)\sin(\alpha + \eta)}{\cos(\alpha)}\right]^2 \sin^2(Sz), \tag{3.50a}$$

$$P_2(z) = \sin^2(\alpha)\cos^2(Sz) + \sin^2(\eta)\sin^2(Sz). \tag{3.50b}$$

The coupling length and the maximum power transfer are of the same form as those defined for the conventional CMT, as is the phase-matching condition for the complete power transfer.

The power exchange between the two waveguides can also be viewed as a consequence of the beating of the symmetriclike and the antisymmetriclike composite modes of the coupler. Suppose that the two waveguides are synchronized, i.e., $\delta = 0$. By using a rigorous mode-matching analysis at the input and the output, we find the output powers from guide 1 and 2 to be

$$P_1(z) = R_s^2 + R_a^2 + 2R_sR_a \cos[(\beta_s - \beta_a)z], \tag{3.51a}$$

$$P_2(z) = R_s^2 + R_a^2 - 2R_sR_a \cos[(\beta_s - \beta_a)z], \tag{3.51b}$$

$$R_s = \frac{\langle 1|s\rangle\langle a|1\rangle}{\langle 1|1\rangle\langle s|s\rangle}, \tag{3.52a}$$

$$R_a = \frac{\langle 1|a\rangle\langle a|1\rangle}{\langle 1|1\rangle\langle a|a\rangle}, \tag{3.52b}$$

which are the excitation ratios of the waveguide mode to the composite modes. $\langle i|j\rangle$ with $i, j = 1, 2, s, a$ stand for the overlap integrals between the different modes:

$$\langle i|j\rangle = \frac{1}{4}\int (\mathbf{e}_i^* \times \mathbf{h}_j + \mathbf{e}_j \times \mathbf{h}_i^*) \cdot \hat{z}\,\mathrm{d}a. \tag{3.53}$$

At the coupling distance (i.e., half of the beat length),

$$L_c = \frac{\pi}{\beta_s - \beta_a}, \tag{3.54}$$

maximum power transfer is

$$P_2|_{\max} = (R_s + R_a)^2, \tag{3.55}$$

where the power remaining in guide 1 is

$$P_1|_{\min} = (R_s - R_a)^2. \tag{3.56}$$

Figures 7(a) and 7(b) show the coupling lengths as functions of separation for the two waveguide structures examined in Figs. 4 and 5, respectively. From Fig. 7(a) it can be observed that the coupling length of the identical waveguides predicted by the nonorthogonal CMT (dashed curves) is in excellent agreement with that produced by the self-consistent orthogonal CMT (or the conventional CMT in this case). One can understand this by noting that the coupling length is related to the difference between $\beta_s$ and $\beta_a$ (or $S$). The coupling length therefore is not affected by the cross power $X$ as much as by the individual propagation constants shown in Fig. 2. Hence, when the two waveguides are similar and not too closely coupled, the simple conventional CMT gives an excellent approximation of the power-transfer length. On the other hand, from Fig. 7(b) it can be noted that the accuracy of the coupling length predicted by the orthogonal CMT decreases as the two waveguides become dissimilar. At the same time, a similar decrease in accuracy by the nonorthogonal CMT can also be observed.

One consequence of the nonorthogonal CMT and the exact normal-mode analysis is the prediction of cross talk in the directional coupler device.[83–86] According to the coupled-mode analysis, the extinction ratio for the output power is equal to

$$\text{E.R.} = X^2, \tag{3.57}$$

whereas the normal mode analysis yields

$$\text{E.R.} = \left(\frac{R_s - R_a}{R_s + R_a}\right)^2. \tag{3.58}$$

Equation (3.58) indicates that the cross talk is caused by the unequal excitation of the two normal modes of the coupler, an issue first raised by Chen and Wang[85] and discussed further by Haus and Whitaker.[86] The extinction

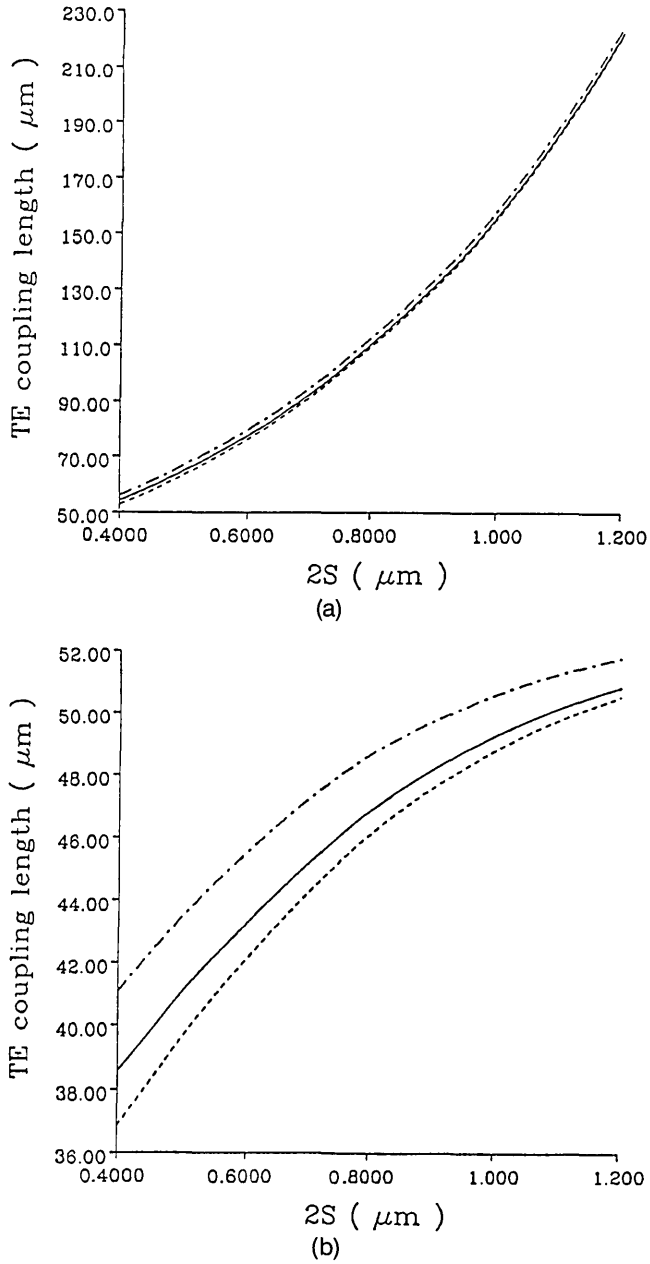


Fig. 7. Coupling lengths as functions of separation for the TE modes of a slab coupler. Solid curves, exact solutions; dashed curves, nonorthogonal CMT; dashed–dotted curves, orthogonal CMT. (a) Identical waveguides shown in Fig. 4, (b) dissimilar waveguides shown in Fig. 5.

ratios calculated with Eqs. (3.57) (dashed curve, coupled-mode analysis) and (3.58) (solid curve, normal-mode analysis) are depicted in Fig. 8 as a function of separation for the TE modes of the parallel slab coupler shown in Fig. 4.

It should be emphasized that the prediction of cross talk based on Eqs. (2.57) and (2.58) implies two separate destructive measurements, each with the other waveguide truncated. Consequently the sum of the guided power in the two individual waveguides $P_1 + P_2$ may not be equal to the total input power. This is not a violation of the law of power conservation but a reflection of the definition assumed for the powers in the individual waveguides shown in Fig. 6. An experimental setup for measuring the guided powers in the individual waveguides according to this definition is described in Ref. 81. In reality the situations may be different from what has been assumed in this definition, and one should be cautious in applying the theory to the prediction of the cross talk in directional couplers.

### F. Limitations and Extensions

The accuracy and validity of the coupled-mode theory described above depend on the trial solutions assumed in Eqs. (3.28). Although the propagation constants of the composite modes calculated by the CMT are stationary values and thus are insensitive to errors in the trial solutions, the field patterns are not. Generally speaking, one restriction is that the separation between the waveguides not be too small. The accuracies in both propagation constants and field patterns deteriorate as the separation decreases, as shown in Figs. 4 and 5. This so-called weak-coupling limitation may be overcome to some extent by use of a variational principle under the scalar approximation.[40]

Another restriction is that the index discontinuities across different media not be too large. For the parallel directional coupler shown in Fig. 1 the vector mode in individual waveguide 1 satisfies the boundary conditions only at its core–cladding interfaces. In the presence of waveguide 2 trial solution $\mathbf{e}_1$ may not satisfy the boundary condition at the core–cladding interfaces of guide 2, as in the case of the TM modes in a slab coupler. Therefore the polarization effect (or the vector nature) is considered only partially in the vector coupled-mode formulations. This inconsistency of the vector CMT was first pointed out by Snyder and co-workers.[24,25,28,33] As a result of this inconsistency, the polarization effects may not be properly treated by the CMT. As shown in Refs. 25 and 28, erroneous results were predicted by the nonorthogonal CMT for the power-coupling length of the TM modes when the index discontinuity was large. One solution that is suitable for not-too-strongly guided waveguides is to use the scalar formulation plus a vector correction.[4,41] Another

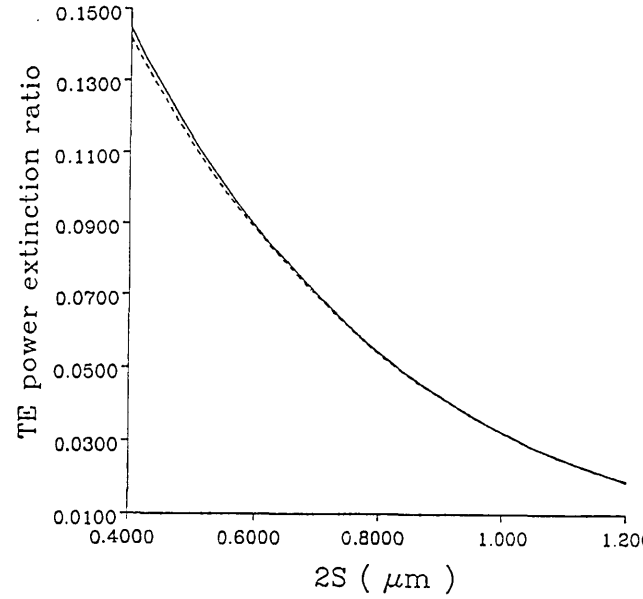


Fig. 8. Power extinction ratios as functions of separation for the TE modes of a slab coupler. Solid curve, exact solution; dashed curve, nonorthogonal CMT. The parameters are the same as those in Fig. 4.

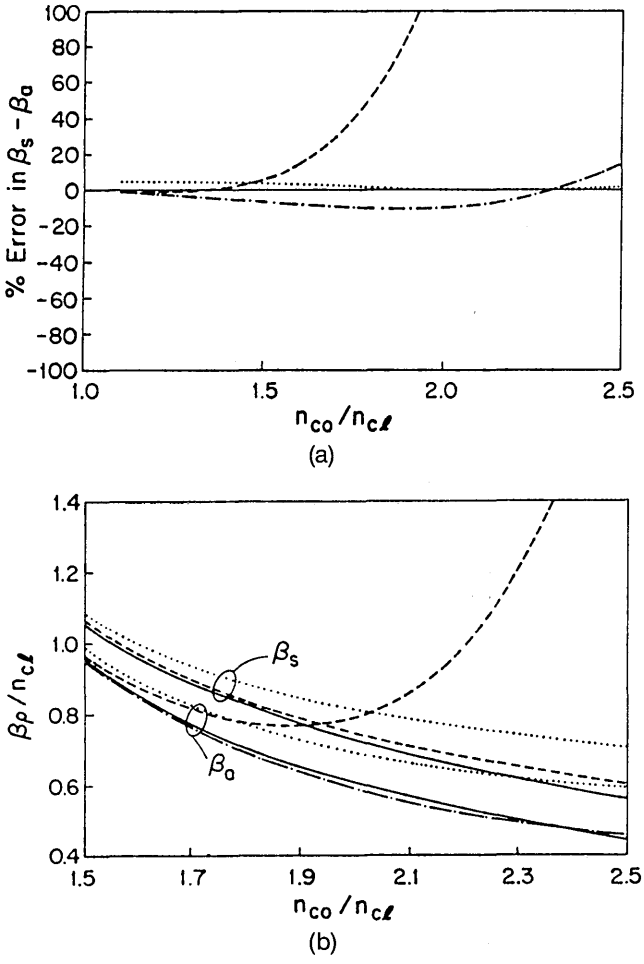


Fig. 9. (a) Percentage errors in the coupling lengths for the TM modes of parallel slabs, (b) effective indices of the TM modes of parallel slabs. Curves are taken from Ref. 35. $\beta$ is the propagation constant, $\rho$ is the width of the slab, and $n_{cl}$ is the refractive index of the cladding.

approach that may be applied to strongly guided waveguides is to introduce improved trial solutions. A modified coupled-mode formulation has been developed based such a new trial solution, in which the previously neglected polarization effect is considered[35]; and the same trial solution was used by Ankiewicz *et al.* in conjunction with a perturbation analysis.[33] Significant improvement in accuracy over the original trial solution was observed for the TM modes of strongly guided waveguides. So far the improved trial solutions are found only for some simple waveguide structures; a systematic coupled-mode approach to the strongly guided coupled waveguides is still lacking.

Figure 9(a) displays the percentage errors in the difference of the propagation constants of the normal TM modes as functions of the ratio of core and cladding indices. The curves are taken from Ref. 35. It is noted that the nonorthogonal CMT is more accurate than the conventional one when the index difference is small. On the other hand, the nonorthogonal CMT gives erroneous results for a large index difference, whereas the conventional theory seems globally accurate. An improvement in the performance of the nonorthogonal CMT with modified trial function can be observed. The effective indices of the even and the odd modes are also calculated by the three theories and are plotted in Fig. 9(b). It is shown that neither the conventional nor the nonorthogonal CMT's, which are based on the vector modes of the individual waveguides, are accurate when the index discontinuities become large, whereas the modified trial functions indeed indicate substantial improvement.[35]

## 4. COUPLED-MODE FORMULATIONS FOR GRATING-ASSISTED COUPLERS

Directional couplers made of uniform waveguides can couple light between guides only when the waveguide modes are phase matched or nearly so. For single-mode waveguides, this means that the two waveguides have to be similar, if not identical. Grating-assisted couplers, on the other hand, may achieve power coupling between two modes (or guides) that are originally not phase matched. In general, directional couplers that are subject to periodic index perturbations along the direction of the wave propagation represent an important class of directional coupler devices. Examples of grating-assisted couplers include optical wavelength filters[87] and tunable lasers,[88] both demonstrated by Alferness and coworkers at the AT&T Bell Laboratories. A configuration of the grating-assisted coupler is depicted in Fig. 10. Two dissimilar parallel waveguides are placed in close proximity. A periodic index corrugation is distributed along the waveguide axis. The role of the periodic grating is to assist the coupling process for efficient power exchange between the asynchronous waveguides.

### A. Conventional Coupled-Mode Formulation

The conventional coupled-mode formulations established in Section 3.A have no explicit assumptions about the nature of the modes and the couplings between them. The propagation constants and the coupling coefficients may be either independent of $z$ (ideal modes) or $z$ varying (local modes). For the grating-assisted couplers, the coupling coefficients $K_{ij}$ are no longer independent of $z$ but are periodic functions of $z$. Suppose that the period of the grating is $\Lambda$. One can expand the coupling coefficients in terms of Fourier series,

$$K_{ij} = \sum_{-\infty}^{+\infty} C_{ij}^{m} \exp\left(-j\frac{2m\pi}{\Lambda}z\right), \tag{4.1}$$

where $C_{ij}^{m}$ is the $m$th Fourier coefficient. By substitution of Eq. (4.1) into Eqs. (3.2), one can derive a set of coupled-

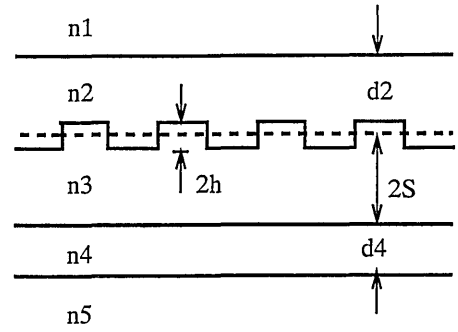


Fig. 10. Schematic diagram of a grating-assisted coupler.

mode equations:

$$\frac{da_1}{dz} = -j(\beta_1 + C_{11}{}^0)a_1 - jC_{12}{}^{+m}\exp\left(-j\frac{2m\pi}{\Lambda}z\right)a_2, \tag{4.2a}$$

$$\frac{da_2}{dz} = -j(\beta_2 + C_{22}{}^0)a_2 - jC_{21}{}^{-m}\exp\left(+j\frac{2m\pi}{\Lambda}z\right)a_2. \tag{4.2b}$$

In the derivation of Eqs. (4.2), only phase-matching terms are retained. Define

$$a_1 = \hat{a}_1\exp\left(-j\frac{\beta_1 + C_{11}{}^0 + \beta_2 + C_{22}{}^0}{2}z\right)\exp\left(-j\frac{m\pi}{\Lambda}z\right), \tag{4.3a}$$

$$a_2 = \hat{a}_2\exp\left(-j\frac{\beta_1 + C_{11}{}^0 + \beta_2 + C_{22}{}^0}{2}z\right)\exp\left(+j\frac{m\pi}{\Lambda}z\right). \tag{4.3b}$$

Then Eqs. (4.2) are reduced to Eqs. (3.7), with a new detuning factor defined by

$$\delta = \frac{\beta_1 + C_{11}{}^0 - \beta_2 - C_{22}{}^0}{2} - \frac{m\pi}{\Lambda} \tag{4.4}$$

and a modified coupling coefficient

$$\kappa = C_{12}{}^{+m} = C_{21}{}^{-m}. \tag{4.5}$$

It is noted that only dc components in the self-coupling coefficients contribute to the detuning factors, whereas the coupling between the two modes depends on the phase-matched ac components in the mutual coupling coefficients.

The results obtained from the solutions of the conventional coupled-mode equations in Section 3.A are directly applicable to the analysis of the grating-assisted couplers. By following similar arguments for uniform couplers, one can readily show that complete power transfer between the two dissimilar waveguides may still be achieved at the coupling length determined by Eq. (4.5) if the grating period $\Lambda$ is chosen so as to nullify the detuning in Eq. (4.4). These predictions are valid, however, only when the waveguides are far apart and very different, as shown in Subsection 4.C below. The power-coupling process in the grating-assisted couplers is dictated by two distinct coupling mechanisms: (1) the natural coupling between two waveguides similar to that in the uniform directional couplers and (2) the periodic coupling that is due to the grating perturbations. The approximate CMT analysis considers only the coupling that is due to the gratings and therefore may not be sufficient when the two waveguides are not far from synchronism and are not far apart.

### B. Nonorthogonal Coupled-Mode Formulation

For the grating-assisted couplers the refractive index may be expressed as

$$n^2(x,y,z) = \bar{n}^2(x,y) + \Delta n^2(x,y)\sum_{-\infty}^{+\infty}F_m\exp\left(-j\frac{2m\pi}{\Lambda}z\right), \tag{4.6}$$

where $\bar{n}$ is the refractive index of a uniform (i.e., $z$-invariant) reference structure and the second term represents a periodic index perturbation that is due to the grating.

We express the unknown fields in the grating-assisted coupler by a linear superposition of the ideal waveguide modes, as in Eqs. (3.28). In addition to the conditions stated in Section 2 for the uniform couplers, the perturbations that are due to the index grating are assumed to be small. The coupled-mode equations are derived from the complex-power theorem[47] and take the same form as Eq. (3.35) except that the coupling matrix contains both the natural coupling between the waveguides and the periodic coupling that is due to the grating. One may separate the total coupling matrix into two terms:

$$\mathbf{H} = \bar{\mathbf{H}} + \tilde{\mathbf{K}}, \tag{4.7}$$

where $\bar{H}_{ij}$ is defined in Eqs. (3.30)–(3.32). The matrix $\tilde{\mathbf{K}}$ is the coupling that is due to the presence of the grating,

$$\tilde{K}_{ij} = \frac{1}{4}\omega\epsilon_0\sum_{-\infty}^{\infty}F_m\exp\left(-j\frac{2m\pi}{\Lambda}z\right)\int\Delta n^2\mathbf{e}_i^*\cdot\mathbf{e}_j da. \tag{4.8}$$

Since $\mathbf{P}$ and $\bar{\mathbf{H}}$ are independent of $z$, one may diagonalize them by using a method similar to that presented in Subsection 4.A. By applying Eqs. (3.16) and (3.39), one may reduce the coupled-mode equations to

$$\frac{d}{dz}\mathbf{W} = -j\mathbf{B}\mathbf{W} - j\mathbf{L}\mathbf{W}, \tag{4.9}$$

where $\mathbf{W}$ and $\mathbf{B}$ are the matrices for the amplitudes and the propagation constants, respectively, of the composite modes of the uniform coupler.

$$\mathbf{L} = \mathbf{O}^t\tilde{\mathbf{K}}\mathbf{O} \tag{4.10}$$

is the coupling matrix between the composite modes that are due to the index grating. By using Eqs. (3.38) and (3.43), one can readily derive the following expressions for the coupling coefficients:

$$L_{ij} = \frac{1}{4}\omega\epsilon_0\sum_{-\infty}^{\infty}F_m\exp\left(-j\frac{2m\pi}{\Lambda}z\right)\int\Delta n^2\mathbf{e}_i^*\cdot\mathbf{e}_j da, \tag{4.11}$$

where $i,j = s,a$ for the symmetriclike and the antisymmetriclike modes, which can be expressed as a linear combination in terms of the waveguide modes, as in Eqs. (3.43). If the coupler is lossless, then the power conservation requires that the coupling matrix be Hermitian, i.e., that

$$L_{sa} = L_{as}{}^*. \tag{4.12}$$

Equations (4.9) and (4.11) take forms identical to those obtained directly from a trial solution that is based on the linear superposition of the exact composite modes of the parallel coupler.[90,92] The only difference is that the composite modes here are represented by a linear combination of the waveguide modes, an approximation that is valid if the two waveguides are not very closely coupled or strongly guided.

### C. Solutions to the Coupled-Mode Equations

In comparison with the coupled-mode formulations for the waveguide modes, Eq. (4.7) contains only the coupling that is due to the grating perturbation. In fact Eq. (4.9) is identical to the conventional coupled-mode equations (3.2) and hence may be solved in a manner similar to that given in Subsection 4.A. Without loss of generality we assume that the grating is of rectangular shape and is used to match the first-order spatial harmonics (i.e., $m = \pm 1$). We derive a transfer matrix that links the amplitudes for the composite modes between two positions along $z$:

$$\mathbf{W}(z) = \mathbf{T}_W(z)\mathbf{W}(0), \tag{4.13}$$

where

$$t_{11}^W = [\cos(Qz) - j\cos(\phi)\sin(Qz)]\exp[-j(\pi/\Lambda)z], \tag{4.14a}$$

$$t_{12}^W = \sin(\phi)\sin(Qz)\exp[-j(\pi/\Lambda)z], \tag{4.14b}$$

$$t_{21}^W = -\sin(\phi)\sin(Qz)\exp[j(\pi/\Lambda)z], \tag{4.14c}$$

$$t_{22}^W = [\cos(Qz) + j\cos(\phi)\sin(Qz)]\exp[j(\pi/\Lambda)z], \tag{4.14d}$$

where

$$Q = (\delta_W^2 + \kappa_W^2)^{1/2}, \tag{4.15}$$

$$\tan(\phi) = \kappa_W/\delta_W, \tag{4.16}$$

with

$$\delta_W = (\beta_s - \beta_a)/2 - \pi/\Lambda \tag{4.17}$$

being the detuning factor and

$$\kappa_W = \frac{1}{2\pi}\omega\epsilon_0 \int \Delta n^2 \mathbf{e}_s^* \cdot \mathbf{e}_a \, da \tag{4.18}$$

being the coupling coefficient.

The phase-matching condition $\delta_W = 0$ yields the optimum grating period,

$$\Lambda_W = \pi/(\beta_s - \beta_a). \tag{4.19}$$

Furthermore, if the two waveguides are highly dissimilar and weakly coupled, the natural coupling between the two waveguides may be neglected, so that Eq. (4.19) reduces to

$$\Lambda_A = \pi/(\beta_1 - \beta_2), \tag{4.20}$$

which is the result from application of the conventional CMT presented in Subsection 4.A.

Comparisons between the two phase-matching conditions in Eqs. (4.19) and (4.20) are made for a grating-assisted coupler consisting of slab waveguides. The parameters are $n_1 = 1.0$, $n_2 = 3.3$, $n_3 = 3.2$, $n_4 = 3.5$, and $n_5 = 3.0$; $d_2 = 1.0$ $\mu$m, $d_4 = 0.3$ $\mu$m, and $2s = 0.6$ $\mu$m. The wavelength is $\lambda = 1.5$ $\mu$m. The grating is placed along the core–cladding interface of the upper slab (see Fig. 10). Figure 11 illustrates the grating periods predicted by the two different phase-matching conditions (dashed curve, $\Lambda_W$; dashed–dotted line, $\Lambda_A$) as functions of the waveguide separation. The phase-matching grating period that is based on the predicted composite modes by Eq. (4.19) increases as the separation becomes larger, whereas the one based on the waveguide modes given in Eq. (4.20) is independent of the separation. These two grating periods are quite different when the two waveguides are close, and Eq. (4.20) is valid only if the separation is very large. For the sake of comparison, we also plotted the calculated grating period that is based on the exact composite modes (solid curve). It can be seen that the nonorthogonal CMT indeed produces very accurate results for the grating period.

Under the phase-matching condition [Eqs. (4–19)], the transfer matrix becomes

$$\mathbf{T}_W = \begin{bmatrix} \cos(\kappa_W z)\exp[-j(\pi/\Lambda)z] & \sin(\kappa_W z)\exp[-j(\pi/\Lambda)z] \\ \sin(\kappa_W z)\exp[+j(\pi/\Lambda)z] & -\cos(\kappa_W z)\exp[+j(\pi/\Lambda)z] \end{bmatrix}. \tag{4.21}$$

At the input and the output the amplitudes of the composite modes should be related to those of the waveguide modes so that the power exchange between the waveguides may be examined. Assume that the coupling length is equal to an integer number of grating periods, i.e., that

$$L_c = N\Lambda. \tag{4.22}$$

The transfer matrix for the amplitudes of the waveguide modes is

$$\mathbf{T}_A = \mathbf{O}\mathbf{T}_W\mathbf{O}^{-1} = \frac{1}{\cos(\alpha)} \begin{bmatrix} \cos(\kappa_W L_c - \alpha) & \sin(\kappa_W L_c) \\ \sin(\kappa_W L_c) & \cos(\kappa_W L_c + \alpha) \end{bmatrix}. \tag{4.23}$$

Suppose that, at the input, only guide 1 is excited. The guided powers in guides 1 and 2, respectively, are given by

$$P_1(L_c) = \cos^2(\kappa_W L_c), \tag{4.24a}$$

$$P_2(L_c) = \sin^2(\kappa_W L_c - \alpha). \tag{4.24b}$$

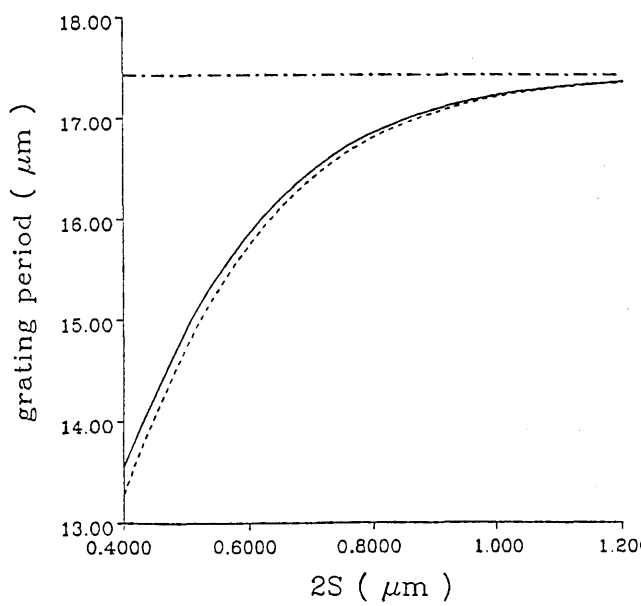


Fig. 11. Phase-matching periods as functions of separation for the TE modes of a slab coupler. Parameters: $n_1 = 1.0$, $n_2 = 3.3$, $n_3 = 3.2$, $n_4 = 3.5$, and $n_5 = 3.0$; $d_2 = 1.0$ $\mu$m, $d_4 = 0.3$ $\mu$m, $2S = 0.6$ $\mu$m. $\lambda = 1.5$ $\mu$m. Solid curve, exact; dashed curve, nonorthogonal CMT; dashed–dotted curve, conventional orthogonal CMT.

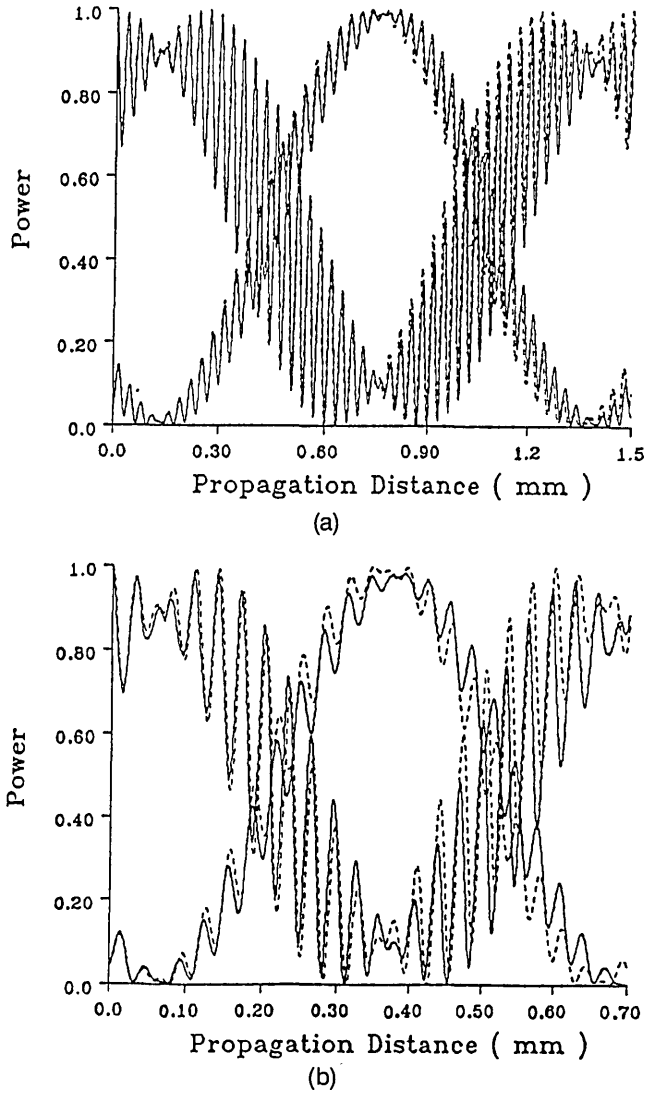


Fig. 12. Power exchange as a function of $z$. Solid curves, finite-difference BPM; dashed curves, nonorthogonal CMT. (a) $2h = 0.1$ $\mu$m, (b)$2h = 0.2$ $\mu$m. The parameters are the same as those in Fig. 11.

The complete power transfer occurs at

$$L_{\max} = \frac{\pi/2 + \alpha}{\kappa_W}, \tag{4.25}$$

which is different from the prediction of the conventional CMT. According the nonorthogonal CMT, the maximum power-transfer length is related to the coupling between the composite modes as well as to the cross power between the two guides. Zero cross talk may also be achieved at a different coupling length,

$$L_{\min} = \pi/(2\kappa_W). \tag{4.26}$$

Similar results have been obtained by application of a multiple-scale analysis[53] for a sinusoidal grating and of a transfer matrix for a rectangular grating.[52]

The power coupling in the grating-assisted coupler is calculated by use of the nonorthogonal coupled-mode formulations developed above; the results are shown in Fig. 12 by solid curves. The same structure as that used in Fig. 11 is assumed. The separation between the two slabs is $2s = 0.6$ $\mu$m. The height of the grating is $2h = 0.1$ $\mu$m and $2h = 0.2$ $\mu$m in Figs. 12(a) and 12(b), respectively. The two distinct coupling scales are clearly illustrated in both cases. The slow scale, which dictates the overall power coupling, is determined by the coupling of the grating. The two coupling lengths for the maximum power transfer and the minimum cross talk are also shown. The fast scale is due to the natural coupling between the two parallel uniform waveguides. The period of the fast oscillation is equal to $\Lambda$, and its magnitude is related to the strength of the natural coupling between the two waveguides. If the two waveguides are far from synchronism and are far apart, then the natural coupling may be ignored. In this limit the conventional CMT discussed in Subsection 3.A applies. To assess the accuracy of the coupled-mode theory, I simulated the same structure by using a beam-propagation method[89] (BPM, dashed curves). Better agreement between the two methods is observed for the case depicted in Fig. 12(a) than for the case depicted in Fig. 12(b). When the grating perturbation is strong the trial solutions in the CMT are no longer accurate, resulting in larger errors. In addition the radiation loss becomes more pronounced as the grating height increases, which is illustrated in the BPM simulations; this effect is absent in the coupled-mode analysis. Nevertheless, the principal features of the grating-assisted couplers revealed by the CMT are verified by the BPM simulations. Although the simple conventional CMT is not reliable for the grating-assisted coupler, as shown in Refs. 50 and 90, a modified self-consistent orthogonal CMT was shown to yield accurate results when the two waveguides were not strongly coupled.[91] Instead of using Eq. (4.5) for the coupling and Eqs. (3.24) for the power exchange, one may use the self-consistent orthogonal CMT developed in Eq. (3.4) to obtain the expressions for the composite modes, i.e., Eqs. (3.45) and (3.46). Then one may utilize the formulations developed in Subsection 4.C to obtain expressions for the composite modes, i.e., Eqs. (3.45) and (3.46), and apply the formulations developed in Subsection 4.C for the grating-assisted couplers. Under this circumstance the only difference between the nonorthogonal and the orthogonal theories results from the differences in the propagation constants and the field patterns of the composite modes, which have been discussed in great detail in Subsection 3.D. The difference in the propagation constants will affect the accuracy of the phase-matching grating period in Eq. (4.19), whereas the difference in the field patterns may cause errors in the coupling lengths, as can be seen from Eqs. (4.18), (4.25), and (4.26).

### E. Limitations and Extensions

As in the case of the uniform couplers, the accuracy and validity of the coupled-mode analysis for the grating-assisted couplers are determined by the accuracy and validity of the trial solutions assumed in Eqs. (3.28). First, the separation between the waveguides cannot be too small. To overcome this limitation, one may use the exact composite modes of the parallel waveguides as the basis for the trial solutions.[90,92] Second, the grating perturbation, for example, the grating height, must be small. In our trial solutions the ideal modes are used so that the

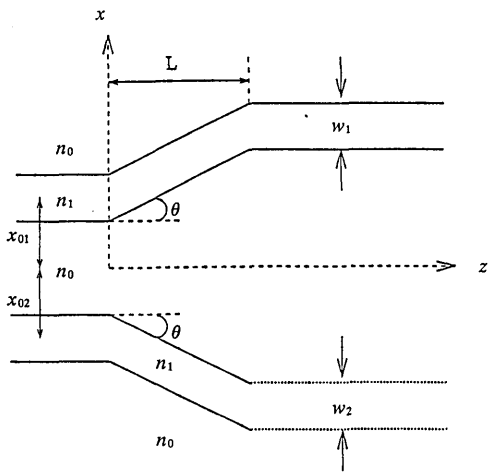


Fig. 13. Schematic diagram of a tapered coupler.

mode profiles will not change along $z$. Furthermore, the index differences among different media must be small. This problem may be partially solved by use of the composite modes, but the index discontinuities associated with the grating perturbation should still be small.[93] Finally, the radiation caused by the grating has been ignored in the above CMT analysis. The radiation loss may be included in the analysis by consideration of the coupling between the guided and the radiation modes.[94] Recently a transfer-matrix method (TMM) based on the local composite modes was applied to the grating-assisted couplers.[95] It was demonstrated that the TMM is capable of simulating grating-assisted couplers that have strong natural coupling and grating perturbations; it can treat the polarization in a strongly guided structure properly; it can estimate the power attenuation that is due to the radiation loss. If only the guided modes are employed in the analysis, the TMM usually overestimates the loss that is due to the radiation modes, because of the omission of the radiative power that is coupled back to the guided modes. This problem can be solved by inclusion of the radiation modes.[96] In general the TMM appears to be superior to the CMT that is based on the ideal modes. An improved formulation achieved by use of the local normal modes as the trial solutions is expected to overcome the shortcomings of the CMT that is based on the ideal modes,[97] but it is yet to be demonstrated for the grating-assisted couplers.

## 5. COUPLED-MODE FORMULATIONS OF TAPERED COUPLERS

Tapered couplers or nonparallel waveguides are used in optical directional couplers for the purpose of reducing cross talk,[86] improving fabrication tolerance, increasing bandwidth,[98] and suppressing filter sidelobes.[99] Since the overall performance of the couplers, including transmission, cross talk, and extinction ratio, is often critically affected by the characteristics of the tapered or the nonparallel sections, it is important to undertake a rigorous analysis of the power exchange between the tapered and the nonparallel waveguide structures.

A typical tapered coupler consists of two or more tapered or nonparallel waveguides. The taper may be caused by the variation of the refractive index or the geometric shape of the waveguides and can be characterized by a refractive index $n(x, y, z)$ that varies with $x$, $y$, and $z$. Figure 13 shows a tapered coupler made of two nonparallel straight waveguides separating at an angle $\theta$. Because of the longitudinal nonuniformity a rigorous analysis of the tapered optical couplers is difficult. In the coupled-mode theory the fields in the tapered coupler are represented approximately as a linear superposition of the local modes. The local modes are the normal modes of the uniform waveguide structures defined at each point along the $z$ axis, as depicted in Fig. 14. The local modes are not solutions of the Maxwell's equations for the tapered structures; rather, they are modal solutions of the local uniform waveguides with $z$-varying parameters.

### A. Conventional Coupled-Mode Formulations

One can readily extend the conventional coupled-mode equations to the tapered couplers by making the propagation constants and the coupling coefficients functions of $z$. To solve the coupled-mode equations with $z$-varying coefficients requires numerical integrations. One important case in which an analytical solution can be obtained is that in which the two waveguides are synchronized throughout the entire coupling region. By applying Eq. (3.16) to Eq. (3.9) with $\delta = 0$ and

$$\mathbf{O} = \begin{bmatrix} 1/\sqrt{2} & -1/\sqrt{2} \\ 1/\sqrt{2} & 1/\sqrt{2} \end{bmatrix}, \tag{5.1}$$

we derive a transfer matrix for the mode amplitudes:

$$\mathbf{T} = \begin{bmatrix} \cos\left(\int_0^z \kappa dz'\right) & -j \sin\left(\int_0^z \kappa dz'\right) \\ -j \sin\left(\int_0^z \kappa dz'\right) & \cos\left(\int_0^z \kappa dz'\right) \end{bmatrix}. \tag{5.2}$$

Therefore complete power exchange between the two waveguides can still be achieved, and the coupling length

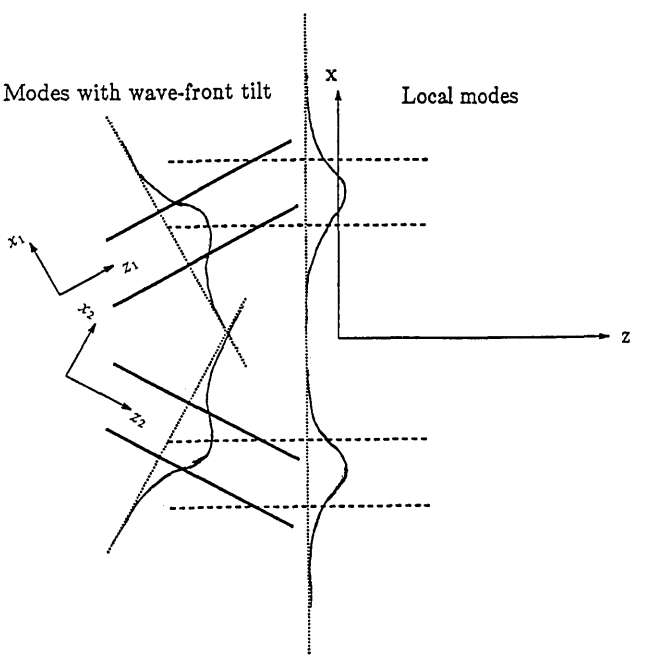


Fig. 14. Illustration of the local modes used in the coupled-mode formulations.

is determined by

$$\int_0^{L_c} \kappa \mathrm{d}z = \frac{\pi}{2}. \tag{5.3}$$

### B. Nonorthogonal Coupled-Mode Formulations

The rigorous coupled-mode formulations can be derived by assuming that the total electromagnetic fields in the tapered couplers can be expressed as a linear superposition of the two local modes of the individual waveguides defined at $z$:

$$\mathbf{E}(x,y,z) = a_1(z)\mathbf{e}_1(x,y;z) + a_2(z)\mathbf{e}_2(x,y;z),$$
$$\mathbf{H}(x,y,z) = a_1(z)\mathbf{h}_1(x,y;z) + a_2(z)\mathbf{h}_2(x,y;z). \tag{5.4}$$

Expansion (5.4) is a good approximation if local guided modes exist in the entire coupling region and the two waveguides are not very closely coupled or strongly guided. We also assume that the taper varies slowly so that the coupling to the radiation modes or the effect of wavefront tilt may be neglected.

The coupled-mode equations governing the evolution of expansion coefficients $a_1(z)$ and $a_2(z)$ can be derived by substitution of Eqs. (5.4) into Maxwell's equations.[63] In matrix form the equations are written as

$$\mathbf{P}\frac{\mathrm{d}}{\mathrm{d}z}\mathbf{A} = -j\overline{\mathbf{H}}\mathbf{A} - \mathbf{F}\mathbf{A}, \tag{5.5}$$

where $\overline{H}_{ij}$ and $P_{ij}$ are of the same forms as those defined in Eqs. (3.29)–(3.31). For the tapered couplers they become $z$ dependent. In addition a new coupling term appears in the coupled-mode equations:

$$F_{ij} = \frac{1}{4}\int\left(\mathbf{e}_i^* \times \frac{\partial \mathbf{h}_j}{\partial z} + \frac{\partial \mathbf{e}_j}{\partial z} \times \mathbf{h}_i^*\right)\cdot \hat{z}\,\mathrm{d}a, \tag{5.6}$$

representing the additional coupling caused by the taper. It has been shown that $F_{ij}$ are essential for the self-consistency of the nonorthogonal coupled-mode equations [Eqs. (5.5)].[63] Even for a very slow taper, $F_{ij}$ should not be neglected; otherwise the law of power conservation will be violated. It is also shown below that a self-consistent adiabatic approximation for slowly tapered couplers may be introduced in conjunction with the orthogonal coupled-mode formulation that is based on the local composite modes.

The coupled-mode equations for the orthogonal local composite modes can be derived from Eqs. (5.5) by the same linear transformation as given in Eqs. (3.16) and (3.37). In matrix form, Eqs. (5.5) are reduced to

$$\frac{\mathrm{d}}{\mathrm{d}z}\mathbf{W} = -j\mathbf{B}\mathbf{W} - \mathbf{N}\mathbf{W}, \tag{5.7}$$

where the local composite modes are given in terms of the linear superposition of the local waveguide modes that are determined by Eqs. (3.43). The coupling coefficients are obtained as

$$\mathbf{N} = \mathbf{M}^+\mathbf{P}\frac{\mathrm{d}}{\mathrm{d}z}\mathbf{M} + \mathbf{M}^+\mathbf{F}\mathbf{M}. \tag{5.8}$$

By imposing the condition for the power conservation, one can easily prove that the coupling coefficients are antisymmetric, i.e., that

$$N_{\mathrm{sa}} = -N_{\mathrm{as}}^*, \tag{5.9}$$

and that the diagonal elements $N_{\mathrm{ss}} = N_{\mathrm{aa}} = 0$. This result is to be expected: since the coupling matrix in Eqs. (5.7) is real, its diagonal elements must be zero; otherwise the power would be lost or generated, and thus the law of power conservation would be violated. It is also evident that the additional coupling terms $F_{ij}$ are essential for ensuring the self-consistency of the coupled-mode formulation.

The orthogonal coupled-mode equations [Eqs. (5.7)] can also be derived from Maxwell's equations when the fields in the tapered couplers are represented by the linear superposition of the exact local composite modes.[63,100,101] The coupling coefficients result solely from the tapering effect and are given by

$$N_{\mathrm{sa}} = \frac{1}{4}\int\left(\mathbf{e}_s^* \times \frac{\partial \mathbf{h}_a}{\partial z} + \frac{\partial \mathbf{e}_a}{\partial z} \times \mathbf{h}_s^*\right)\cdot \hat{z}\,\mathrm{d}a, \tag{5.10}$$

where $\mathbf{e}_s$, $\mathbf{h}_s$, and $\mathbf{e}_a$, $\mathbf{h}_a$ are the fields of the local composite modes. By using the linear transformations (3.16) and (3.43), one may readily derive Eq. (5.10) from Eq. (5.8). Evaluation of the coupling coefficients between the local composite modes with use of Eq. (5.8) or Eq. (5.10) is cumbersome. An alternative expression for the coupling coefficient may be derived[3]:

$$N_{\mathrm{sa}} = \frac{1}{4}\frac{\omega\epsilon_0}{\beta_s - \beta_a}\int \frac{\partial n^2}{\partial z}\mathbf{e}_s^* \cdot \mathbf{e}_a \mathrm{d}a. \tag{5.11}$$

Note that the coupling between the local composite modes is proportional to the rate of change in the refractive index along $z$. If the taper is very slow then the coupling between the local composite modes may be neglected, and a self-consistent coupled-mode formulation under the adiabatic approximation is obtained. In general, however, the coupling that is due to taper should be considered, and its effect on the power exchange between the guides should be carefully examined.

### C. Power Exchange in the Tapered Couplers

For the synchronous couplers in which the local modes of the waveguides have the same propagation constants, there is no coupling between the local composite modes; i.e., $N_{\mathrm{sa}} = 0$. Thus Eqs. (5.7) can be integrated to yield exact solutions.[60] Assuming that $a_1(0) = 1$ and $a_2(0) = 0$, the mode amplitudes at $z$ may be expressed as

$$a_1(z) = \frac{1}{2}\left\{\left[\frac{1 - X(0)}{1 - X(z)}\right]^{1/2} + \left[\frac{1 + X(0)}{1 + X(z)}\right]^{1/2}\right\}\cos\left(\frac{1}{2}\phi\right) + j\frac{1}{2}\left\{\left[\frac{1 - X(0)}{1 - X(z)}\right]^{1/2} - \left[\frac{1 + X(0)}{1 + X(z)}\right]^{1/2}\right\}\sin\left(\frac{1}{2}\phi\right), \tag{5.12a}$$

$$a_2(z) = \frac{1}{2}\left\{\left[\frac{1 - X(0)}{1 - X(z)}\right]^{1/2} + \left[\frac{1 + X(0)}{1 + X(z)}\right]^{1/2}\right\}\cos\left(\frac{1}{2}\phi\right) - j\frac{1}{2}\left\{\left[\frac{1 - X(0)}{1 - X(z)}\right]^{1/2} - \left[\frac{1 + X(0)}{1 + X(z)}\right]^{1/2}\right\}\sin\left(\frac{1}{2}\phi\right), \tag{5.12b}$$

where

$$\phi = \int_0^z \left(\frac{\beta_s - \beta_a}{2}\right) dz' \tag{5.13}$$

and $\beta_s, \beta_a$ are the propagation constants of the symmetric and the antisymmetric local composite modes and are given by Eqs. (3.45) and (3.46).

When the waveguides are not synchronous, exact analytical solutions are known only for certain cases in which some special relations among $\beta_s$, $\beta_a$, and $N_{sa}$ hold.[6,97] In general the coupled-mode equations may be solved by use of a numerical technique. The amplitudes of the waveguide modes are obtained by means of linear transformation (3.16) and the power in guides 1 and 2 by Eq. (3.49). If the two guides are very far apart at $z = L$, the cross power $X$ may be neglected, so that

$$P_1(L) \approx |a_1(L)|^2, \tag{5.13a}$$

$$P_2(L) \approx |a_2(L)|^2. \tag{5.13b}$$

Therefore the cross talk between the two guides may be greatly reduced by introduction of the tapered section in the output port of the directional couplers.[86]

To examine the power coupling in a tapered coupler, my colleagues and I studied a coupler made of two straight step-index slab waveguides separating at an angle $2\theta$ (see Fig. 13). The input conditions are assumed to be $a_1(0) = 1$ and $a_2(0) = 0$. The parameters of the waveguides are $n_1 = n_2 = 3.1$, $n_0 = 3.0$, $w_1 = 0.8$ $\mu$m, and $w_2 = 0.6$ $\mu$m. The initial separation between the slabs is $x_{01} = 0.55$ $\mu$m and $x_{02} = -0.45$ $\mu$m. The wavelength is $\lambda = 1.5$ $\mu$m. Figures 15(a) and 15(b) show the guided power in guide 1 as a function of the propagation distance $l$ for two tilt angles, $\theta = 0.1°$ and $\theta = 0.5°$, respectively. The solid curves represent the solutions that include the tapering effect, the dashed curves the solutions under adiabatic approximation, and the dotted curves the solutions that simply neglect $F_{ij}$. When the tilt angle is small, the adiabatic solutions appear to be accurate. As the angle increases [as in Fig. 15(b)], the tapering effect becomes important, and the adiabatic solutions are no longer adequate. The solutions that ignore $F_{ij}$ are not correct even when the tilt angle is small. A closer examination reveals that the solutions in fact do not obey the law of power conservation and thereby are not self-consistent.

### D. Limitations and Extensions

Almost all the limitations of the nonorthogonal coupled-mode formulations stated for the uniform and the grating-assisted couplers apply to the tapered couplers. Similarly, some of the problems associated with these limitations may be solved by the methods suggested for the former two types. An additional restriction of the CMT for tapered couplers is that the tapering rate has to be slow so that the wavefront-tilt effect caused by the nonparallel waveguide structures can be ignored. For the tapered coupler shown in Fig. 13 the wave front of the guided mode of each waveguide is perpendicular to its own axis, while the wave front of the local modes (local waveguide modes or composite modes) is perpendicular to $z$. When the tilt angle is small the local-mode approximation is acceptable. For large tilt angles the wavefront-tilt effect in nonparallel waveguides may become important and should be considered.

A self-consistent coupled-mode formulation that accounts for the wavefront-tilt effect was proposed recently.[65,66] In the new formulation the trial solutions are a linear superposition of the normal modes, instead of the local modes, in the tilted individual waveguides. The wavefront-tilt effect also occurs at the input and the output where the transition from the parallel to the nonparallel sections (or vice-versa) occurs. The wavefront tilt is caused by the change of waveguide axes and can be ana-

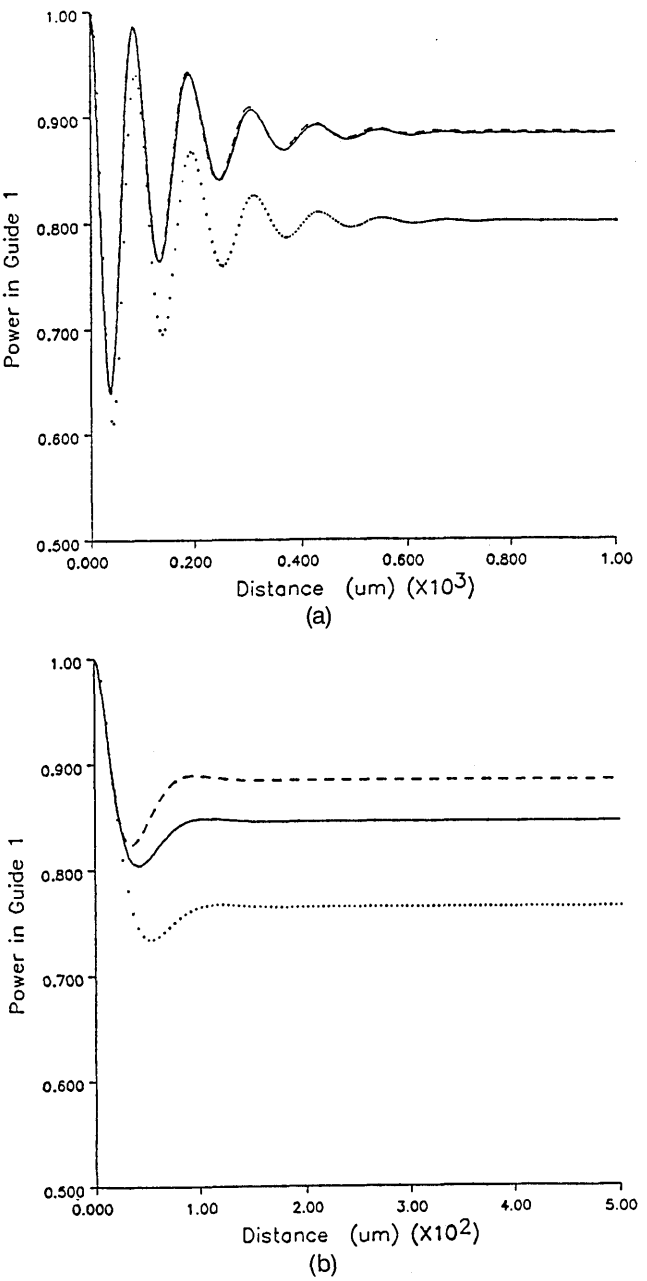


Fig. 15. Guided power in guide 1 as a function of propagation distance $L$. The parameters are $n_1 = n_2 = 3.1$, $n_0 = 3.0$, $w_1 = 0.8$ $\mu$m, and $w_2 = 0.6$ $\mu$m. $x_{01} = 0.55$ $\mu$m, and $x_{02} = 0.45$ $\mu$m. The wavelength is $\lambda = 1.5$ $\mu$m. (a) $\theta = 0.1°$, (b) $\theta = 0.5°$. Solid curves, nonorthogonal CMT with tapering effect; dashed curves, nonorthogonal CMT that neglects $N_{sa}$; dotted curves, nonorthogonal CMT that neglects $F_{12}$.

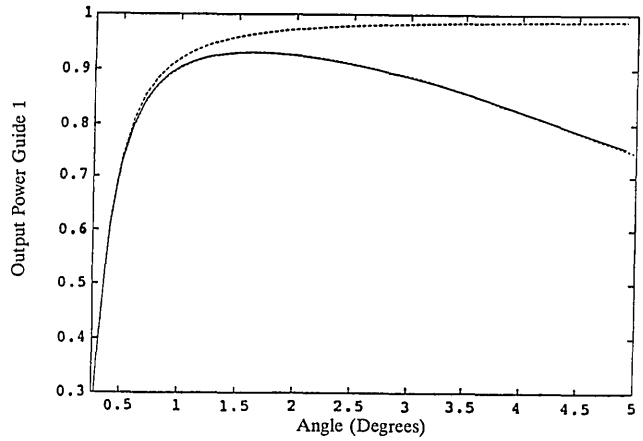


Fig. 16. Output power from guide 1 as a function of tilt angle. The parameters are the same as those in Fig. 14 except that $w_2 = w_1 = 0.8$ $\mu$m, $x_{01} = -x_{02} = 0.7$ $\mu$m. The propagation distance is $L = 200$ $\mu$m. Solid curve, nonorthogonal CMT that considers the wavefront-tilt effect; dashed–dotted curve, nonorthogonal CMT based on the local waveguide modes; dashed curve, finite-difference BPM.

lyzed by the mode matching at the interfaces.[65] Figure 16 shows the output power in guide 1 at $L = 200$ $\mu$m as a function of tilt angle $\theta$. It can be seen that the coupled-mode formulation that is based on the local waveguide modes can yield a reliable prediction only for a tilt angle less than 1°, whereas the improved CMT that includes the wavefront-tilt effect is in excellent agreement with the finite-difference BPM simulation up to 5°. Therefore the improved theory should be used for large tilt angles.

## 6. CONCLUSIONS

The coupled-mode formulations for the optical coupled-waveguide systems are reviewed. The conventional coupled-mode formulations are set up in a simple, heuristic way and are applied to the analysis of both uniform and nonuniform structures. The rigorous coupled-mode formulations are established by use of a linear superposition of the modes of the individual waveguides as a trial solution to Maxwell's equations. The cross-power terms, which were ignored in the conventional CMT, show up naturally in the rigorous CMT as a result of the nonorthogonality between the waveguide modes. The cross power is necessary for the self-consistency of the coupled-mode formulations when the coupled waveguides are not phase matched. It also leads to the prediction of the cross talk in the directional couplers. A self-consistent orthogonal coupled-mode formulation can be derived from the nonorthogonal CMT if one neglects the cross power, but the coupling coefficients are redefined as the average of the two mutual coupling coefficients. This self-consistent orthogonal CMT is simpler than the improved nonorthogonal CMT and is reliably accurate for describing the power exchange between waveguides that are weakly coupled. A more appropriate approach to orthogonalizing the CMT that is based on the waveguide modes is to apply a linear transformation that simultaneously diagonalizes the power and the natural coupling matrices. The resultant orthogonal CMT is equivalent to the coupled-mode formulations based on the ideal or the local composite modes, except that the composite modes are approximated by a linear superposition of the modes of the individual waveguides or waveguide modes.

Three typical coupler configurations—the uniform coupler, the grating-assisted coupler, and the tapered coupler—are analyzed in detail. For the uniform coupler discussed in Section 2 the nonorthogonal coupled-mode equations are diagonalized by the linear transformation, and the composite modes are the normal modes of the system. The power exchange between the waveguides may be treated either by coupling between the waveguide modes or by beating between the composite modes. It is shown that the nonorthogonal CMT in general yields highly accurate dispersion relations and field patterns if the separation between the waveguides is not too small and the index discontinuities over the cross section are not too large. Extensions of the CMT for the analysis of strongly coupled or guided waveguides are also discussed.

In the grating-assisted coupler two different coupling mechanisms exist for the waveguide modes: the natural coupling between the two waveguides and the periodic coupling that is due to the grating. After the linear transformation the coupled-mode equations for the composite modes contain the coupling that is due to the periodic gratings only and may be solved approximately under a quasi-phase-matching condition. The optimum grating period is determined by the phase-matching condition of the composite modes other than that of the waveguide modes. The power coupling exhibits two distinct scales that are due to the two coupling mechanisms.

The coupled-mode equations for the tapered coupler are established on the basis of the local waveguide modes. It is noted that not only do the power and the natural coupling matrices become dependent on $z$ but also an additional coupling term appears that is due to the taper. This extra coupling is essential for the self-consistency of the CMT and may not be ignored, even under the adiabatic condition. The nonorthogonal CMT can be orthogonalized by the linear transformation, and the orthogonal CMT that is based on the local composite modes contains only the coupling that is due to the taper. If the taper is slow the tapering effect may be neglected and an approximate solution may be obtained. In general the tapering effect should be considered, and the coupled-mode equations have to be solved numerically. One of the major shortcomings of the CMT that is based on the local modes is that the wavefront-tilt effect is ignored. This wavefront-tilt effect may be considered by use of an improved coupled-mode formulation.

Several limitations of the coupled-mode theory for the analysis of optical coupled-waveguide systems are pointed out, and some of the existing approaches to overcoming these restrictions are mentioned. In general, one can always use a complete set of the modes as a trial solution. The coupled-mode equations derived are an infinite number of coupled ordinary differential equations and may be subsequently solved numerically. From this point of view the coupled-mode theory may be considered a rigorous numerical method. Nevertheless, one should bear in mind that the appealing characteristic of the CMT for optical guided waves lies in its simplicity and intuitiveness. Typical longitudinal dimensions of optical waveguides are usually much larger than the waveguide wavelengths of

optical signals. The interactions between the optical waves and the guiding media generally are weak. As a result the couplings between optical guided waves per wavelength are weak. For any significant interactions to occur, the phase-matching conditions between the interacting waves must be satisfied. A precise description of this resonant coupling phenomenon is indeed the essence of the coupled-mode theory.

## ACKNOWLEDGMENTS

The author expresses his gratitude to H. A. Haus of the Massachusetts Institute of Technology for his encouragement, guidance, and insight throughout the research work related to the subject of this paper. The author acknowledges the comments and suggestions of W. K. Burns, A. W. Snyder, and S. L. Chuang. Thanks also go to J. Hong for calculations related to the uniform and the grating-assisted couplers, to B. E. Little and S. Lessard for calculations for the tapered couplers, and to C. L. Xu for the BPM simulations. Financial support from the Natural Sciences and Engineering Research Councils of Canada and the National Science Foundation of the United States is acknowledged.

## REFERENCES

1. H. A. Haus and W. P. Huang, "Coupled-mode theory," Proc. IEEE **79,** 1505–1518 (1991).
2. D. L. Lee, *Electromagnetic Principle of Integrated Optics* (Wiley, New York, 1986).
3. D. Marcuse, *Theory of Dielectric Optical Waveguides*, 2nd ed. (Academic, New York, 1991).
4. A. W. Snyder and J. D. Love, *Optical Waveguide Theory* (Chapman & Hall, London, 1983).
5. H. A. Haus, *Waves and Fields in Optoelectronics* (Prentice-Hall, Englewood Cliffs, N.J. 1984).
6. T. Tamir, ed., *Guided-Wave Optoelectronics* (Springer-Verlag, New York, 1988).
7. Y. R. Shen, *Principles of Nonlinear Optics* (Wiley, New York, 1984).
8. G. P. Agrawal, *Nonlinear Fiber Optics* (Academic, Boston, Mass., 1989).
9. J. R. Pierce, "Coupling of modes of propagation," J. Appl. Phys. **25,** 179–183 (1954).
10. S. E. Miller, "Coupled wave theory and waveguide applications," Bell Syst. Tech. J. **33,** 661–719, (1954).
11. S. A. Schelkunoff, "Conversion of Maxwell's equations into generalized telegraphist's equations," Bell Syst. Tech. J. **34,** 995–1043 (1955).
12. H. A. Haus, "Electron beam waves in microwave tubes," in *Proceedings of the Symposium on Electronic Waveguides* (Polytechnic Institute of Brooklyn, Brooklyn, N.Y., 1958).
13. A. W. Snyder, "Coupled-mode theory for optical fibers," J. Opt. Soc. Am. **62,** 1267–1277 (1972).
14. D. Marcuse, "Coupled mode theory of round optical fibers," Bell Syst. Tech. J. **52,** 817–842 (1973).
15. A. Yariv, "Coupled-mode theory for guided-wave optics," IEEE J. Quantum Electron. **QE-9,** 919–933 (1973).
16. H. Kogelnik, "Theory of dielectric waveguides," in *Integrated Optics*, T. Tamir, ed. (Springer-Verlag, New York, 1975), Chap. 2.
17. H. Kogelnik, "Switched directional couplers with alternating $\Delta\beta$," IEEE J. Quantum Electron. **QE-12,** 396–401 (1976).
18. H. Kogelnik and C. V. Shank, "Coupled-wave theory of distributed feedback lasers," J. Appl. Phys. **43,** 2327–2335 (1972).
19. A. Hardy and W. Streifer, "Coupled-mode theory of parallel waveguides," J. Lightwave Technol. **LT-3,** 1135–1146 (1985).
20. H. A. Haus, W. P. Huang, S. Kawakami, and N. A. Whitaker, "Coupled mode theory of optical waveguides," J. Lightwave Technol. **LT-5,** 16–23 (1987).
21. S. L. Chuang, "A coupled mode formulation by reciprocity and a variational principle," J. Lightwave Technol. **LT-5,** 5–15 (1987).
22. W. Streifer, M. Osinski, and A. Hardy, "Reformulation of coupled-mode theory of multiwaveguide systems," J. Lightwave Technol. **LT-5,** 1–4 (1987).
23. C. Vassello, "About coupled-mode theories for dielectric waveguides," J. Lightwave Technol. **6,** 294–303 (1988).
24. A. W. Snyder and A. Ankiewicz, "Fibre couplers composed of unequal cores," Electron. Lett. **22,** 1237–1238 (1988).
25. A. W. Snyder, A. Ankiewicz, and A. Altintas, "Fundamental error of recent coupled mode formulations," Electron. Lett. **23,** 1097–1098 (1987).
26. W. Streifer, "Coupled mode theory," Electron. Lett. **23,** 216–217 (1987).
27. W. Streifer, "Comment on 'Fundamental error of recent coupled mode formulations,'" Electron. Lett. **22,** 718–719 (1988).
28. A. W. Snyder, A. Ankiewicz, and A. Altintas, "Coupled mode theory neglects polarization phenomena" (reply to Ref. 26), Electron. Lett. **22,** 720–721 (1988).
29. W. Streifer, M. Osinski, and A. Hardy, "A critical review of coupled mode theory," in *Integrated Optical Circuit Engineering V*, M. A. Mentzer, ed., Proc. Soc. Photo-Opt. Instrum. Eng. **835,** 178 (1987).
30. A. Hardy, W. Streifer, and M. Osinski, "Weak coupling of parallel waveguides," Opt. Lett. **13,** 162–163; erratum, 428 (1988).
31. Y. Wu, "Discussion of HS formulation using equivalent current theory," Electron. Lett. **24,** 376–377 (1988).
32. Z. H. Wang and S. R. Seshadri, "Asymptotic theory of guided modes in two parallel, identical dielectric waveguides," J. Opt. Soc. Am. A **5,** 782–792 (1988).
33. A. Ankiewicz, A. Altintas, and A. W. Snyder, "Polarization properties of evanescent couplers," Opt. Lett. **13,** 524–525 (1988).
34. A. W. Snyder, Y. Chen, and A. Ankiewicz, "Coupled waves on optical fibers by power conservation," J. Lightwave Technol. **7,** 1400–1406 (1989).
35. H. A. Haus, W. P. Huang, and A. W. Snyder, "Coupled-mode formulations," Opt. Lett. **14,** 1222–1224 (1989).
36. C. Vassallo, "Condensed formula for coupling coefficients between parallel dielectric waveguides," Electron. Lett. **23,** 304–306 (1986).
37. E. Marcatili, "Improved coupled-mode equations for dielectric guides," IEEE J. Quantum Electron. **QE-22,** 988–993 (1986).
38. A. W. Snyder, "Optical fiber couplers—optimum solution for unequal cores," J. Lightwave Technol. **6,** 463–474 (1988).
39. R. R. A. Syms and R. G. Peall, "Explanation of asymmetric switch response of three-arm directional couplers in Ti:$LiNbO_3$ using strong coupling theory," Opt. Commun. **66,** 260–264 (1988).
40. W. P. Huang and S. K. Chaudhuri, "Variational coupled-mode theory of optical couplers," J. Lightwave Technol. **8,** 1565–1570 (1990).
41. W. P. Huang, S. T. Chu, and S. K. Chaudhuri, "A scalar coupled-mode theory with vector correction," J. Quantum Electron. **28,** 184–193 (1992).
42. A. Hardy and W. Streifer, "Coupled modes of multiwaveguide systems and phased arrays," J. Lightwave Technol. **LT-4,** 90–99 (1986).
43. S. L. Chuang, "A coupled-mode theory for multiwaveguide systems satisfying the reciprocity theorem and power conservation," J. Lightwave Technol. **LT-5,** 174–183 (1987).
44. A. Hardy and W. Streifer, "Analysis of phased-array diode lasers," Opt. Lett. **10,** 335–337 (1985).
45. A. Hardy and W. Streifer, "Coupled-mode solutions of multiwaveguide systems," IEEE J. Quantum Electron. **QE-22,** 528–534 (1986).
46. Y. Shama, A. Hardy, and E. Marom, "Multimode coupling of unidentical waveguides," J. Lightwave Technol. **7,** 420–425 (1989).

47. A. Hardy, W. Streifer, and M. Osinski, "Coupled-mode equations for multimode waveguide systems in isotropic or anisotropic media," Opt. Lett. **11,** 742–744 (1986).
48. F. Tian, Y. Z. Wu, and P. A. Ye, "Improved coupled-mode theory for anisotropic waveguide modulators," IEEE J. Quantum Electron. **24,** 531–536 (1988).
49. L. Tsang and S. L. Chuang, "Improved coupled-mode theory for reciprocal anisotropic waveguides," J. Lightwave Technol. **6,** 304–311 (1988).
50. W. P. Huang and H. A. Haus, "Power exchange in grating-assisted couplers," J. Lightwave Technol. **7,** 920–924 (1989).
51. W. P. Huang, B. E. Little, and S. K. Chaudhuri, "A new approach to grating-assisted couplers," J. Lightwave Technol. **9,** 721–727 (1991).
52. W. P. Huang and W. Y. Lit, "Nonorthogonal coupled-mode theory of grating-assisted codirectional couplers," J. Lightwave Technol. **9,** 845–852 (1991).
53. B. E. Little, W. P. Huang, and S. K. Chaudhuri, "A multiple-scale analysis of grating-assisted couplers," J. Lightwave Technol. **10,** 1254–1263 (1992).
54. G. Griffle, M. Itzkovich, and A. A. Hardy, "Coupled-mode formulations for directional couplers with longitudinal perturbation," IEEE J. Quantum Electron. **28,** 985–994 (1992).
55. G. Griffle and A. Yariv, "Frequency response and tunability of grating-assisted directional couplers," IEEE J. Quantum Electron. **27,** 1115–1118 (1991).
56. W. P. Huang, B. E. Little, and C. L. Xu, "On phase-matching and power coupling in grating-assisted couplers," IEEE Photon. Technol. Lett. **4,** 151–153 (1992).
57. R. R. A. Syms, "Improved coupled-mode theory for codirectionally and contradirectionally coupled waveguide arrays," J. Opt. Soc. Am. A **8,** 1062–1069 (1991).
58. J. Hong and W. P. Huang, "Contra-directional coupling in grating-assisted guided-wave devices," J. Lightwave Technol. **10,** 873–881 (1992).
59. A. Hardy, M. Osiński, and W. Streifer, "Application of coupled-mode theory to nearly parallel waveguide systems," Electron. Lett. **22,** 1249–1250 (1986).
60. R. G. Peall and R. R. A. Syms, "Scalar strong coupled mode theory for slowly-varying waveguide arrays," Opt. Commun. **67,** 421–424 (1988).
61. H. A. Haus and W. P. Huang, "Mode coupling in tapered structures," J. Lightwave Technol. **7,** 729–730 (1989).
62. Y. Cai, T. Mizumoto, and Y. Naito, "Analysis of the coupling characteristics of a tapered coupled waveguide system," J. Lightwave Technol. **8,** 90–98 (1990).
63. W. P. Huang and H. A. Haus, "Self-consistent vector coupled-mode theory for tapered optical waveguides," J. Lightwave Technol. **8,** 922–926 (1990).
64. W. P. Huang and B. E. Little, "Power exchange in tapered optical couplers," IEEE J. Quantum Electron. **27,** 1932–1938 (1992).
65. W. P. Huang and S. Lessard, "Wavefront-tilt in nonparallel optical waveguides," J. Lightwave Technol. **10,** 316–322 (1992).
66. S. Lessard and W. P. Huang, "Assessment of coupled-mode theory for tapered optical coupler," J. Lightwave Technol. **11,** 405–407 (1993).
67. Y. Chen, "Solutions to full coupled wave equations of nonlinear coupled systems," IEEE J. Quantum Electron. **25,** 2149–2153 (1989).
68. S. L. Chuang, "Application of the strongly coupled-mode theory to integrated optical devices," IEEE J. Quantum Electron. **QE-23,** 499–509 (1987).
69. J. P. Donnelly, H. A. Haus, and N. Whitaker, "Symmetric three-guide optical coupler with nonidentical center and outside guides," IEEE J. Quantum Electron. **QE-23,** 401–406 (1987).
70. J. P. Donnelly, L. A. Molter, and H. A. Haus, "The extinction ratio in optical two-guide coupler $\Delta\beta$ switches," IEEE J. Quantum Electron. **25,** 924–932 (1989).
71. Y. Shama, E. Marom, and A. Hardy, "Analysis of power transfer in nonsymmetric directional couplers," Appl. Opt. **28,** 990–994 (1989).
72. R. R. A. Syms and R. G. Peall, "The digital optical switch: analogous directional coupler devices," Opt. Commun. **68,** 235–238 (1989).
73. Y. Tomabechi and K. Matsumura, "Improved analysis for the coupling characteristics of two rectangular dielectric waveguides laid in different layers," IEEE J. Quantum Electron. **24,** 2359–2361 (1988).
74. A. Hardy, S. Shakir, and W. Streifer, "Coupled-mode equations for two weakly guiding single-mode fibers," Opt. Lett. **14,** 324–336 (1986).
75. J. R. Qian, "Generalized coupled-mode equations and applications to fiber couplers," Electron. Lett. **22,** 304–306 (1986).
76. A. Ankiewicz, A. W. Snyder, and X. Zheng, "Coupling between parallel optical fiber cores—critical examination," J. Lightwave Technol. **LT-4,** 1317–1323 (1986).
77. H. S. Huang and H. C. Chang, "Vector coupled-mode analysis of coupling between two identical optical fiber cores," Opt. Lett. **14,** 90–92 (1989).
78. H. S. Huang and H. C. Chang, "Analytical expressions for the coupling between two optical fiber cores with $\alpha$-power refractive-index distribution," J. Lightwave Technol. **7,** 694–702 (1989).
79. H. S. Huang and H. C. Chang, "Analysis of optical fiber directional coupling based on the $HE_{11}$ modes. Part I: the identical-core," J. Lightwave Technol. **8,** 823–831 (1990).
80. H. S. Huang and H. C. Chang, "Analysis of optical fiber directional coupling based on the $HE_{11}$ modes. Part II: the nonidentical-core," J. Lightwave Technol. **8,** 832–837 (1990).
81. E. A. J. Marcatili, L. L. Buhl, and R. C. Alferness, "Experimental verification of the improved coupled-mode equations," Appl. Phys. Lett. **49,** 1692–1693 (1986).
82. R. G. Peall and R. R. A. Syms, "Comparison between strong coupling theory and experiment for three-arm directional couplers in Ti:$LiNbO_3$," J. Lightwave Technol. **7,** 540–554 (1989).
83. H. A. Haus, "Coupled-mode theory revisited," in *Fiber Optics, Optoelectronics and Laser Applications in Science and Engineering,* Proc. Soc. Photo-Opt. Instrum. Eng. (1986).
84. J. P. Donnelly, H. A. Haus, and L. A. Molter, "Cross power and crosstalk in waveguide couplers," J. Lightwave Technol. **6,** 257–268 (1988).
85. K. Chen and S. Wang, "Cross-talk problems in optical directional couplers," Appl. Phys. Lett. **44,** 166–168 (1984).
86. H. A. Haus and N. A. Whitaker, "Elimination of cross talk in optical directional couplers," Appl. Phys. Lett. **46,** 1–3 (1985).
87. R. C. Alferness, T. L. Kock, L. L. Buhl, F. Storz, F. Heismann, and M. J. R. Martyak, "Grating assisted InGaAsP/InP vertical co-directional coupler filter," Appl. Phys. Lett. **55,** 2011–2013 (1989).
88. R. C. Alferness, U. Koren, L. L. Buhl, B. I. Miller, M. G. Young, T. L. Koch, G. Raybon, and C. A. Burrus, "Broadly tunable InGaAsP/InP laser based on a vertical coupler filter with 57-nm tuning range," in *Integrated Photonics Research,* Vol. 10 of 1992 OSA Technical Digest Series (Optical Society of America, Washington, D.C., 1992), p. 308.
89. W. P. Huang, C. L. Xu, S. T. Chu, and S. K. Chaudhuri, "The finite-difference vector beam propagation method: analysis and assessment," J. Lightwave Technol. **10,** 295–305 (1992).
90. D. Marcuse, "Directional couplers made of nonidentical asymmetrical slabs. Part II: grating-assisted couplers," J. Lightwave Technol. **LT-5,** 268–273 (1987).
91. Y. Chen and A. W. Snyder, "Grating-assisted couplers," Opt. Lett. **16,** 217–219 (1991).
92. W. P. Huang, J. Hong, and Z. M. Mao, "An improved coupled-mode formulation for grating-assisted co-directional couplers," IEEE J. Quantum Electron. (to be published).
93. D. G. Hall, "Coupled-mode theory for corrugated optical waveguides," Opt. Lett. **15,** 619–621 (1990).
94. D. Marcuse, "Radiation loss of grating-assisted directional coupler," J. Lightwave Technol. **8,** 675–684 (1990).
95. W. P. Huang and J. Hong, "A transfer matrix approach based on local modes for coupled waveguides with periodic perturbations," J. Lightwave Technol. **10,** 1367–1374 (1992).

96. J. Willems, J. Haes, R. Baets, G. Sztefka, and H. P. Nolting, "Eigenmode propagation analysis of radiation losses in waveguides with discontinuities and grating-assisted couplers," in *Integrated Photonics Research*, Vol. 10 of 1993 OSA Technical Digest Series (Optical Society of America, Washington, D.C., 1993), p. 229.
97. L. A. Weller-Brophy and D. G. Hall, "Local normal mode analysis of guided mode interactions with waveguide gratings," J. Lightwave Technol. **6,** 1069–1082 (1988).
98. A. Milton and W. K. Burns, "Mode coupling in tapered optical waveguide structures and electro-optic switches," IEEE Trans. Circ. Syst. **CS-26,** 1020–1028 (1979).
99. R. C. Alferness and P. S. Cross, "Filter characteristics of codirectionally coupled waveguides with weighted coupling," IEEE J. Quantum Electron. **QE-14,** 843–847 (1978).
100. A. W. Snyder, "Surface mode coupling along a tapered dielectric rod," IEEE Trans. Antennas Propag. **AP-13,** 821–822 (1965).
101. A. W. Snyder, "Coupling of modes on a tapered dielectric cylinder," IEEE Trans. Microwave Theor. Technol. **MTT-18,** 383–392 (1970).